
Electronic Thesis and Dissertation Repository

4-8-2014 12:00 AM

Functional Anatomy of the Anconeus: Muscle Architecture and Motor Unit Number Estimation

Daniel E. Stevens

The University of Western Ontario

Supervisor

Dr. Charles L. Rice

The University of Western Ontario

Graduate Program in Kinesiology

A thesis submitted in partial fulfillment of the requirements for the degree in Master of Science

© Daniel E. Stevens 2014

Follow this and additional works at: <https://ir.lib.uwo.ca/etd>



Part of the [Anatomy Commons](#), and the [Exercise Physiology Commons](#)

Recommended Citation

Stevens, Daniel E., "Functional Anatomy of the Anconeus: Muscle Architecture and Motor Unit Number Estimation" (2014). *Electronic Thesis and Dissertation Repository*. 1945.

<https://ir.lib.uwo.ca/etd/1945>

This Dissertation/Thesis is brought to you for free and open access by Scholarship@Western. It has been accepted for inclusion in Electronic Thesis and Dissertation Repository by an authorized administrator of Scholarship@Western. For more information, please contact wlsadmin@uwo.ca.

**Functional Anatomy of the Anconeus: Muscle Architecture and Motor Unit
Number Estimation**

(Thesis Format: Integrated Article)

By

Daniel E. Stevens

Graduate Program in Kinesiology

A thesis submitted in partial fulfillment
of the requirements for the degree of
Master of Science

The School of Graduate and Postdoctoral Studies
The University of Western Ontario
London, Ontario, Canada

© Daniel E. Stevens

2014

ABSTRACT

Exploring muscle architecture *in vivo* and estimating the number of MUs in the human anconeus muscle have important implications related to the neuromuscular function of this muscle as a model for study in health and disease. The two studies presented in this thesis investigate the functional anatomy of the anconeus in 10 healthy young men (25 ± 3 y).

Ultrasound imaging has facilitated the measure of the architectural variables, fascicle length (L_F) and pennation angle (PA), in many human skeletal muscles *in vivo*. However, the functional anatomy of the anconeus has been investigated mainly from cadavers exclusively. Thus, the purpose of Chapter 2 was to evaluate, using ultrasonography, the degree of change in architectural features, L_F and PA, of the anconeus at rest, across the full range of motion for the elbow joint. The protocol involved imaging the anconeus at 135° , 120° , 90° , 45° , and 0° of elbow flexion. The results indicate that anconeus muscle architecture is dynamic, with L_F and PA decreasing and increasing, respectively, with extension of the elbow. The values obtained here are more representative of architectural changes at various elbow joint positions than those reported in cadaveric studies.

Motor unit number estimates (MUNE) can be determined electrophysiologically using decomposition-enhanced spike-triggered averaging. To provide the most representative MUNE, muscle activation should equal or exceed the upper limit of MU recruitment to activate the majority of the MU pool. A limitation of muscles studied to date, using DE-STA, is an inability to obtain reliable MUNE at forces higher than $\sim 30\%$ of a maximum voluntary contraction. Unique features of the anconeus muscle may permit MUNE at higher muscle activation levels. Thus, the purpose of Chapter 3 was to estimate the number of functional MUs in the anconeus, using DE-STA, at low (10%), moderate (30%), and higher (50%) relative muscle activation

levels (root-mean-square of maximum voluntary contraction (RMS_{MVC})), to determine the effect of muscle activation on MUNE in this muscle. Low average MUNE of 58, 38, and 25 were found for the low, moderate, and higher muscle activations, respectively. A histogram of the distribution of surface-detected MU potentials and elbow extensor force-EMG relationship suggest the most representative MUNE was obtained at $50\%RMS_{MVC}$.

The main findings of this thesis are that; 1) anconeus muscle architecture is dynamic, 2) anconeus allows for a more representative MUNE derived at higher muscle activation levels, and 3) the high signal-to-noise ratio that has made the anconeus a choice model in the study of MU properties, is more likely attributed to a relatively low number of MUs than minimal absolute change in its muscle architecture with elbow excursion.

CO-AUTHORSHIP STATEMENT

This thesis contains material from a published manuscript (Chapter 3). For this manuscript, Daniel E. Stevens was the first author and Brad Harwood, Geoffrey A. Power, Timothy J. Doherty, and Charles L. Rice were co-authors. All experimental data presented in this thesis were collected, analyzed, and interpreted by Daniel E. Stevens.

ACKNOWLEDGEMENTS

I am very appreciative for my time here at The University of Western Ontario as a graduate student. This experience afforded me many opportunities for both academic and personal growth. I would like to recognize those individuals who guided, motivated, and entertained me along the way.

First and foremost, I must thank my supervisor Dr. Charles Rice. Your continued interest, support, and humour helped create an inviting and productive work environment. I suspect your management style, which emphasizes the importance and benefit of collaboration, is unique amongst research laboratories. Having seen the success and opportunity this provides, it is shocking that a focus on team work is not more commonplace. Thank you so much for making my graduate school experience a memorable and rewarding one.

Geoff Power, Brad Harwood, and Cam Smith. Many thanks to you three for all the time, input, and help you offered over the past two years. My productivity in the Neuromuscular Lab undoubtedly benefited from your involvement. Choice.

To Justin, Demetri, and those aforementioned. Thank you for the good times and for keeping it interesting. One's overall impression, when looking back on previous endeavours, always involves a reflection on friendships made. My graduate experience would have been greatly diminished in your absence. Thank you.

I would be remised not to mention my family and girlfriend. To my brother and parents, your unwavering support over all these years has not gone unnoticed and will not be forgotten. I am truly indebted to you. To Caitlin, thank you for all the trips made to London. Your visits were a welcomed diversion, providing the opportunity to discuss matters outside my research, share an exceptionally made meal, and enjoy some fine vino.

TABLE OF CONTENTS

ABSTRACT.....	ii
CO-AUTHORSHIP STATEMENT	iv
ACKNOWLEDGEMENTS.....	v
TABLE OF CONTENTS.....	vi
LIST OF TABLES.....	viii
LIST OF FIGURES	ix
LIST OF APPENDICIES	x
LIST OF ABBREVIATIONS.....	xi
CHAPTER 1 GENERAL INTRODUCTION	1
1.1 MUSCLE ARCHITECTURE.....	1
1.2 MOTOR UNIT	1
1.3 ANCONEUS.....	2
1.3.1 Anatomy and Function of the Anconeus.....	2
1.3.2 EMG Studies of the Anconeus.....	3
1.3.2.1 Anconeus as a Clinical Model.....	5
1.4 ULTRASOUND	6
1.5 MOTOR UNIT NUMBER ESTIMATION.....	7
1.5.1 DE-STA and MUNE.....	10
1.6 PURPOSES.....	11
1.7 REFERENCES	12
CHAPTER 2 STUDY 1: Muscle Architectural Properties of the Anconeus.....	18
2.1 INTRODUCTION	18
2.2 METHODS	21
2.2.1 Participants.....	21
2.2.2 Experimental Protocol.....	21
2.2.3 Ultrasonography.....	22
2.2.4 Data Reduction and Analysis.....	24

2.2.5 Statistical analysis	27
2.3 RESULTS	28
2.4 DISCUSSION	30
2.5 REFERENCES	35
CHAPTER 3 STUDY 2: Motor Unit Number Estimation of the Anconeus ¹	40
3.1 INTRODUCTION	40
3.2 METHODS	43
3.2.1 Participants	43
3.2.2 Experimental Protocol	43
3.2.3 Data Reduction and Analysis	48
3.2.4 Statistical Analysis	49
3.3 RESULTS	51
3.4 DISCUSSION	56
3.5 REFERENCES	61
CHAPTER 4 GENERAL DISCUSSION AND SUMMARY	67
4.1 LIMITATIONS	68
4.2 FUTURE DIRECTIONS	69
4.3 REFERENCES	72
APPENDIX A	75
APPENDIX B	76
APPENDIX C	77
CURRICULUM VITAE	78

LIST OF TABLES

Table 1. Muscle architecture measurements	28
Table 2. Compound muscle action potential of the anconeus and contractile properties of the elbow extensors.....	52

LIST OF FIGURES

Figure 1. Schematic diagrams of the experimental set up.	22
Figure 2. Ultrasound images of the anconeus.	24
Figure 3. Extrapolation of fascicle length and pennation angle.	26
Figure 4. Relationships between architectural features, fascicle length and pennation angle, and elbow position.	29
Figure 5. Schematic diagram of the experiemntal set up and raw electromyography recordings.	47
Figure 6. Frequency distribution histograms of surface-detected motor unit potential negative-peak amplitudes.	52
Figure 7. Relationship between motor unit number estimates and targe activation levels.	53
Figure 8. Relationship between force and normalized electromyography amplitude.	54

LIST OF APPENDICIES

APPENDIX A. Dissected anconeus	75
APPENDIX B. Ethical approval.....	76
APPENDIX C. Permission to reprint previously published manuscript	77

LIST OF ABBREVIATIONS

- ANOVA – Analysis of variance
- CMAP – Compound muscle action potential
- CV – Coefficient of variation
- DE-STA – Decomposition-enhanced spike-triggered averaging
- DQEMG – Decomposition-based quantitative electromyography
- EMG – Electromyography
- EPPs – Endplate potentials
- FDI – First dorsal interosseous
- IPU – Insertion on posterior face of ulna
- L_F – Fascicle length
- LG – Lateral gastrocnemius
- MEPPs – Miniature endplate potentials
- MG – Medial gastrocnemius
- MU – Motor unit
- MUNE – Motor unit number estimate
- MUP – Motor unit potential
- MVC – Maximum voluntary contraction
- MVE – Maximum voluntary effort
- PA – Pennation angle
- PPt – Potentiated twitch
- Pt – Resting twitch
- PCSA – Physiological cross-sectional area
- RMS – Root-mean-square

ROM – Range of motion

SA – Superficial aponeurosis

SD – Standard deviation

SE – Standard error

S-MUP – Surface-detected motor unit potential

SOL – Soleus

TA – Tibialis anterior

TB – Triceps brachii

VA – Voluntary activation

VL – Vastus lateralis

1.0 GENERAL INTRODUCTION

1.1 MUSCLE ARCHITECTURE

Skeletal muscle architecture is defined as “the arrangement of muscle fibers within a muscle relative to the axis of force generation” (Lieber, 1992). Architectural variability between muscles can explain a substantial degree of differences in muscle force production (Lieber and Friden, 2000).

Two key measures are often reported when assessing skeletal muscle architecture as it might pertain to muscle function. Fascicle length (L_F), which is an estimate of muscle fiber length, is defined as the length of a line coincident with the fascicle between the deep and superficial aponeurosis. Fascicle length indicates the range of lengths over which the muscle is capable of actively producing force, known as the excursion potential (Lieber and Friden, 2000). Fascicle length during submaximal isometric contraction has also been shown to influence MU recruitment and discharge rates in human tibialis anterior (Pasquet et al., 2005). Pennation angle (PA) represents the angle of the muscle fibers that comprise a muscle fascicle, relative to the force-generating axis, and directly affects both the force production and the excursion (Gans and De Vree, 1987) (See Figure 3, Page 26). Together, these architectural parameters can be used to calculate the physiological cross-sectional area (PCSA), a measure that is directly proportional to the maximum force generated by a muscle (Lieber and Friden, 2000).

1.2 MOTOR UNIT

The motor unit (MU), as defined by Liddell and Sherrington (1925), is the smallest functional unit of the neuromuscular system, and is comprised of an anterior horn cell (motor neuron), including its dendrites and axon, together with the muscle

fibers it innervates. The number of muscle fibers innervated by the single motor neuron, known as the innervation ratio, varies across motor unit types and muscles (Enoka, 1995). Muscles are characterized by their MU number and by the differences in their MUs, such as innervation ratio, size of soma, distribution of muscle fibers, and cross-sectional area of the muscle fibers (Enoka, 1995). Activation of a MU (MU recruitment) occurs when the motor neuron is excited and discharges a train of action potentials, which in turn activates the innervated muscle fibers. Motor unit recruitment is dependent upon the ease at which the motor neuron can be discharged synaptically, a function of MU size, with the largest cells requiring higher amounts of excitatory inputs (Henneman, 1957). Once recruited, the intensity of activity of each MU can be varied by modulating the rate and pattern at which it discharges action potentials. By this arrangement, the nervous system can increase muscle force gradually and smoothly by varying the combinations of MU recruitment and modulating MU discharge rate (Adrian and Bonk, 1929; Gilson and Mills, 1943).

1.3 ANCONEUS

1.3.1 Anatomy and Function of the Anconeus

The anconeus is a small (total area = $\sim 2,000\text{mm}^2$), primarily type I (60-67%) (Hwang et al., 2004) muscle, innervated by a branch of the radial nerve, that originates on the dorsal aspect of the lateral epicondyle of the humerus and inserts along the proximal third of the posterior face of the ulna (Coriolano et al., 2009; Molinier et al., 2011). At the point of origin, a tendinous expansion (aponeurosis) arises and extends along the lateral inferior border of the muscle, towards the proximal and middle third of the ulna. At the superficial surface, muscle fibers arise obliquely from the aponeurosis and insert

on the posterior face of the ulna, with fibers arising more obliquely at the proximal end than those more distal (Coriolano et al., 2009; Pereira, 2013; Molinier et al., 2011; Bergin et al., 2013), whereas at the deep surface, muscle fibers fan out from a tendon-like structure at the apex of the muscle (Pereira, 2013). The anconeus muscle is also strongly adhered to the lateral joint capsule of the humeroulnar joint, which may potentially compensate for the absence of a posterior bundle on the lateral collateral ligament, suggesting a major role of the anconeus is to actively stabilize the elbow during extension (Basmajian and Griffin, 1972; Molinier et al., 2011; Pereira, 2013) (see Appendix A). The anconeus also functions to extend the elbow, contributing less than ~15% to maximum elbow extension torque (Zhang and Nuber, 2000), and abduct the ulna during resisted pronation (Gleason et al., 1985; Travill, 1962). These various functions at the elbow and forearm may be attributed to anatomically distinct regions of the anconeus (Bergin et al., 2013).

1.3.2 EMG Studies of the Anconeus

A study examining muscle activity of the extensor apparatus of the forearm was likely the first to investigate the human anconeus muscle using electromyography (EMG) (Travill, 1962). Needle EMG was recorded from the three heads of the triceps brachii (TB) and anconeus during unloaded and loaded slow dynamic forearm extensions, while at various degrees of shoulder flexion, and during free and resisted pronation and supination of the forearm with the elbow flexed 90°. Travill (1962) concluded that the triceps brachii and anconeus can be activated independently of one another, and that regardless of shoulder position or load, the anconeus remained active, demonstrating 'slight' activity at no loads and progressing to 'moderate' and 'marked' as load was

increased. Furthermore, the anconeus was found to be also active during resisted pronation and supination.

Further studies have examined the anconeus in more detail. Harwood et al. (2011) investigated motor unit (MU) discharge rates of the anconeus during loaded velocity-dependent elbow extensions due to its easily accessible location for needle EMG recordings compared with other limb muscles (Pasquet et al., 2006; Abellaneda et al., 2009). Loaded (25% of maximum voluntary contraction (MVC)) elbow extension velocities were performed over a 120° range of motion (ROM) at five target velocities (0%, 25%, 50%, 75%, and 100% of maximum velocity at 25%MVC). Motor unit discharge rates increased as a function of velocity, entering a secondary range of firing as the velocity approached maximum. As a result of successful MU recordings during fast dynamic contractions, attributed to a high signal-to-noise ratio, Harwood and Rice (2012) investigated whether anconeus MU recruitment thresholds, during the torque production phase preceding movement, were affected by the resultant peak velocity. Isotonic dynamic elbow extensions were performed at velocities ranging from 64-500°/s with a constant resistance of 25%MVC. The results were variable, with only 7 of 17 MUs displaying a significant negative MU recruitment threshold-velocity relationship (Harwood and Rice, 2012).

More recently, fine wire EMG was utilized to investigate the MU mechanisms that modulate force during ramped contractions in the anconeus, and lateral and long heads of the TB (Harwood et al., 2013). Recruitment thresholds and corresponding MU discharge rates were tracked during 1s epochs over forces ranging from 0-75%MVC. The anconeus was consistent with its twitch contractile properties and fiber-type

composition, and had lower recruitment thresholds than both heads of the TB (Harwood et al., 2013).

Bergin et al. (2013) proposed that distinct anatomical regions of the anconeus muscle were more active during the performance of different functional tasks. Intramuscular and surface EMG recordings were obtained from two regions of the anconeus (longitudinal and transverse) during pronation-supination of the forearm, elbow flexion-extension while at pronated, supinated, and neutral forearm positions, and while gripping. The results suggest that the longitudinal region of the anconeus contributes to control of ulna abduction during forearm pronation, while both regions are active during elbow extension, the degree of which dependent upon forearm position (Bergin et al., 2013).

1.3.2.1 Anconeus as a Clinical Model

The accessibility of this muscle has been exploited in various clinical assessments of neuromuscular function. Kennett and Fawcett (1993) performed repetitive nerve stimulation of the radial nerve while recording surface EMG signals of the anconeus. After performing a maximal isometric elbow contraction, a bar electrode was used to stimulate the radial nerve at 3Hz, repeated at 5s, 30s, and 60s intervals for 5-6mins. Control studies showed the test to be reliable and well tolerated. For ocular myasthenia, myasthenia gravis, congenital myasthenia, and Lambert-Eaton myasthenic syndrome, repetitive nerve stimulation of the anconeus proved more sensitive than abductor digiti minimi stimulation, but equally sensitive as deltoid (Kennett and Fawcett, 1993). Maselli et al. (1991) examined diseases of neuromuscular transmission by recording intracellular miniature endplate potentials (MEPPs) and endplate potentials (EPPs) from *in vitro*

preparations of the anconeus using microelectrodes. Marked abnormalities were detected in the MEPPs and EPPs recorded from the anconeus muscle biopsies in all patients studied, and minimal surgical discomfort was reported (Maselli et al., 1991). As well, a clinical investigation of radial nerve lesions, electrically stimulated the radial nerve while recording nerve conduction velocity and distal latency values at the anconeus (Gassel and Diamantopoulos, 1964). By using the anconeus, a muscle innervated by a branch of the radial nerve, the authors were better able to diagnose the location of the lesion and follow the course of reinnervation.

1.4 ULTRASOUND

Ultrasound imaging has facilitated the measurement of muscle architectural features at rest, and during static and dynamic contractions, in many human skeletal muscles *in vivo*. For example, L_F and PA of the tibialis anterior (TA) were measured using ultrasonography at four ankle joint angles (-15° , 0° , 15° , and 30°) at rest and during dorsiflexor MVC (Maganaris and Baltzopoulos, 1995). Results indicated that L_F and PA decreased and increased, respectively, when contracted compared to at rest. Similarly, Simoneau et al. (2012) measured change in architectural variables of the TA during isometric dorsiflexion and plantar flexion, with the participant's foot firmly secured in place at a neutral ankle joint position (0°). Maximal isometric ramp contractions were performed for 5s, before slowly relaxing toward resting state. From the ultrasound images, it was determined that L_F decreased and PA increased at higher isometric dorsiflexion contractile intensities. Fukunaga et al. (1997) also observed this relationship in the vastus lateralis (VL) when performing maximal isometric knee extensions at 12 different knee angles, ranging from flexion at 110° to full extension (0°). Furthermore,

Chleboun et al. (2001) demonstrated an inverse relationship between L_F and PA of the human biceps femoris muscle in a relaxed state as a function of nine different hip and knee angles, and went on to show a decrease in L_F for the TA and VL when measured during the swing phase of gait (Chleboun et al., 2007).

A recent systematic review tested the reliability and validity of ultrasound measurements of muscle L_F and PA in humans (Kwah et al., 2013). Thirty-six reliability studies and six validity studies met the inclusion criteria. Data from these studies indicated that ultrasound measurements of L_F and PA were reliable across a broad range of experimental conditions (static and dynamic contractions, and at rest). Based on a small number of validity studies, the limited evidence suggests ultrasound imaging of these architectural variables are valid, at least in the muscles tested, in a static and relaxed state (Kwah et al., 2013).

1.5 MOTOR UNIT NUMBER ESTIMATION

The direct assessment of MU numbers for any muscle or muscle group typically involves the cadaveric measurement of the number of α axons innervating a muscle. This approach requires nerve dissection, myelinated axon counts from a cross-sectional slice of the nerve, axon diameter measurement, and the identification of afferent and efferent axons (Enoka, 1995). Limitations in these cadaveric measurements, such as errors associated with distinguishing between small- and large-diameter axons and between afferent and efferent axons, have created uncertainty over the accuracy of cadaveric values (McComas et al., 1971; Duron et al., 1978; Boyd and Davey, 1968). Furthermore, this technique cannot be applied *in vivo* to study MU numbers in health, disease, and adult aging.

Since the advent of the original electrophysiological method for estimating the number of MUs *in vivo*, based on manual incremental stimulation of a motor nerve (McComas et al., 1971), many improved techniques have evolved and developed. One of these techniques, known as automatic quantitative EMG, utilized the availability of powerful digital signal processing software to decompose EMG signals into its constituent MU potential (MUP) trains (Dorfman and McGill, 1988). These MUP trains represent the firing times of a number of active MUs, and from it, a representative MUP train with standard morphological features, can be extracted. In addition, analysis of the firing times of the constituent MUPs provides information on MU recruitment and serve as a triggering source for identifying surface-detected MUPs (S-MUPs) (Doherty et al., 1995). From this, a motor unit number estimate (MUNE) can be derived. More recently, the development of a system of computer-based algorithms for EMG signal decomposition and quantitative analysis (DQEMG) (Stashuk, 1999) has allowed for faster data acquisition and processing, the ability to obtain MUPs from low and higher recruitment threshold MUs, and the ability to obtain S-MUPs and MU firing rate information (Doherty and Stashuk, 2003).

The same basic principle is utilized in all MUNE techniques: 1) elicitation of a compound muscle action potential (CMAP), representing the total mass action potential of the entire muscle, produced via supramaximal electrical stimulation of the motor nerve to a given muscle; 2) collection of a sample of S-MUPs, from which an average in their mean size is calculated; and 3) derivation of a MUNE by dividing the size-related parameter of the CMAP by that of the mean S-MUP. The difference between the current, various MUNE techniques, including incremental stimulation, multiple point stimulation,

statistical method, and spike-triggered averaging, is the way in which the sample of S-MUPs is collected (Boe et al., 2004). With respect to the method utilized in this thesis, MUNE s derived using decomposition-based spike-triggered averaging (DE-STA) are of interest. The DE-STA technique employs a selective intramuscular electrode and surface electrodes simultaneously to detect EMG signals during isometric contractions at low to moderate intensities. The needle-detected EMG signals are decomposed into individual MUPs using a series of algorithms (Stashuk, 1999), involving detection, initial clustering or classification, and supervised classification of the intramuscular signal (Doherty and Stashuk, 2003). The MUPs are then used as triggering sources, based on MUP shape and firing time, to select specific sections of the surface EMG signal, which are averaged to produce an S-MUP. The mean sizes of the representative S-MUPs are then used to derive a MUNE (Doherty et al., 1995). Regardless of technique, MUNE s cannot be obtained in all muscles, as electrically evoked estimates of single MU amplitudes and CMAP derivation require the electrical stimulation of the nerve innervating the specific muscle, making it difficult to apply these techniques to proximal muscles as they often have relatively inaccessible nerves (Shefner, 2001). Furthermore, because MUNE s derived using DE-STA are limited by the level of EMG signal interference (Boe et al., 2005; Conwit et al., 1997), muscles which undergo relatively large absolute changes in their muscle architecture or movement of the skin over the muscle during contraction are not ideal models, because even low contraction intensities could result in the physical displacement of the indwelling and surface recording electrodes, resulting in increased signal complexity. Despite these limitations, estimates of MU numbers in many limb muscles have proved to be a useful and valuable method in the study of health, disease,

and adult aging (Boe et al., 2005; McNeil et al., 2005; Allen et al., 2013; Dalton et al., 2008; Power et al., 2010; 2012).

1.5.1 DE-STA and MUNE

Decomposition-enhanced spike-triggered averaging has proven to be a reliable and valid technique for estimating the number of MUs in a muscle group (Boe et al., 2004; Doherty et al., 2009). However, DE-STA can be affected by muscle activation level and contractile force. For example, when applied to the vastus medialis during 5%, 10%, 20%, and 30%MVC isometric knee extensions, average S-MUP amplitude was found to increase with force, suggesting that low levels of contraction may result in a biased sampling and small average S-MUP amplitude (Conwit et al., 1997). Boe et al. (2005) examined the effect of force on the physiological characteristics of MUPs and S-MUPs, and the subsequent MUNE obtained from the first dorsal interosseous. Intramuscular and surface-detected EMG signals were collected simultaneously during 30s voluntary isometric contractions performed at 10%, 20%, 30%, 40%, and 50%MVC. Results indicated that with increased levels of contraction, S-MUP amplitude increased, resulting in a subsequent decrease in MUNE (Boe et al., 2005). Similarly, the effect of contraction intensity on MUNE was measured in the TA during isometric dorsiflexion contractions (threshold, 10%, 20%, 30%, and 40%MVC) (McNeil et al., 2005). The authors reported a significant and progressive decline in MUNE with increased contraction intensity, and suggested an ensemble MUNE collected at 25%MVC provided the most representative MU number in the TA, using an average S-MUP based on a sample of both low- and high-threshold MUs.

1.6 PURPOSES

Exploring muscle architecture *in vivo* and estimating the number of MUs in the human anconeus muscle have important implications related to the neuromuscular function of this muscle. The anconeus has proved to be a valuable model in the study of MU properties due to high intramuscular EMG signal clarity over the full range of dynamic elbow extensions (Harwood et al., 2011; 2012a). This could be explained by; 1) minimal physical displacement of the recording electrode due to relatively small absolute changes in its muscle architecture, or 2) MU number estimates of the anconeus are relatively low, manifesting as less electrical interference from adjacent MUs and a less dense signal. Thus, the purpose of Chapter 2 was to evaluate, using ultrasonography, the degree of change in architectural features, L_F and PA, of the anconeus at rest for various static positions across the full ROM (135°) of the elbow joint. Accordingly, Chapter 3 aims to estimate the number of functional MUs in the anconeus, using DE-STA, at low (10%), moderate (30%), and higher (50%) relative muscle activation levels, to determine the effect of varying levels of muscle activation on MUNE in this muscle.

1.7 REFERENCES

- Abellaneda S, Guissard N, Duchateau J. The relative lengthening of the myotendinous structures in the medial gastrocnemius during passive stretching differs among individuals. *J Appl Physiol* 2009; 106:169-177.
- Adrain ED, Bonk DW. The discharge of impulses in motor nerve fibres. Part II. The frequency of discharge in reflex and voluntary contractions. *J Physiol (Lond)* 1929; 67:119-151.
- Allen MD, Choi IH, Kimpinski K, Doherty TJ, Rice CL. Motor unit loss and weakness in association with diabetic neuropathy in humans. *Muscle Nerve* 2013; 48(2):298-300.
- Basmajian JV, Griffin WR. Function of anconeus muscle. An electromyographic study. *J Bone Joint Surg Am* 1972; 54:1712-1714.
- Bergin MJ, Vicenzino B, Hodges, PW. Functional differences between anatomical regions of the anconeus muscle in humans. *J Electromyogr Kinesiol* 2013; 23(6):1391-1397.
- Boe SG, Stashuk DW, Brown WF, Doherty TJ. Decomposition-based quantitative electromyography: effect of force on motor unit potentials and motor unit number estimates. *Muscle Nerve* 2005; 31:365-373.
- Boe SG, Stashuk DW, Doherty TJ. Motor unit number estimation by decomposition-enhanced spike-triggered averaging: control data, test-retest reliability, and contractile level effects. *Muscle Nerve* 2004; 29:693-699.
- Boyd IA, Davey MR. Composition of peripheral nerves. Edinburgh: Livingstone.

- Chleboun GS, Busic AB, Graham KK, Stuckey HA. Fascicle length change of the human tibialis anterior and vastus lateralis during walking. *J Orthop Sports Phys Ther* 2007; 37(7):372-379.
- Chleboun GS, France AR, Crill MT, Braddock HK, Howell JN. In vivo measurement of fascicle length and pennation angle of the human biceps femoris muscle. *Cells Tissues Organs* 2001; 169(4):401-409.
- Conwit RA, Tracy B, Jamison C, McHugh M, Stashuk D, Brown WF, Metter EJ. Decomposition-enhanced spike-triggered averaging: contraction level effects. *Muscle Nerve* 1997; 20(8):976-982.
- Coriolano MGWS, Lins OG, Amorim MJAAL, Amorim AA. Anatomy and functional architecture of the anconeus muscle. *Int J Morph* 2009; 27(4):1009-1012.
- Dalton BH, McNeil CJ, Doherty TJ, Rice CL. Age-related reductions in the estimated numbers of motor units are minimal in the human soleus. *Muscle Nerve* 2008; 38:1108-1115.
- Doherty TJ, Simmons Z, O'Connell B, Felice KJ, Conwit R, Chan KM, Komori T, Brown T, Stashuk DW, Brown WF. Methods for estimating the numbers of motor units in human muscles. *J Clin Neurophysiol* 1995; 12(6):565-584.
- Doherty TJ, Stashuk DW, Boe SG. Decomposition-enhanced spike triggered averaging MUNE: validity, reliability, and impact of contraction force. *Suppl Clin Neurophysiol* 2009; 60:119-127.
- Doherty TJ, Stashuk DW. Decomposition-based quantitative electromyography: methods and initial normative data in five muscles. *Muscle Nerve* 2003; 28:204-211.

- Dorfman LJ, McGill KC. AAEE minimonography #29: automatic quantitative electromyography. *Muscle Nerve* 1988; 11(8):804-818.
- Duron B, Jung-Caillol MC, Marlot D. Myelinated nerve fiber supply and muscle spindles in the respiratory muscles of cat: quantitative study. *Anat Embryol (Berl)* 1978; 152(2):171-192.
- Enoka RM. Morphological features and activation patterns of motor units. *J Clin Neurophysiol* 1995; 12(6):538-559.
- Fukunaga T, Ichinose Y, Ito M, Kawakami Y, Fukashiro S. Determination of fascicle length and pennation in a contracting human muscle in vivo. *J Appl Physiol* 1997; 82(1):354-358.
- Gans C, de Vree F. Functional bases of fiber length and angulation in muscle. *J Morphol* 1987; 192(1):63-85.
- Gassel MM, Diamantopoulos E. Pattern of conduction times in the distribution of the radial nerve. *Neurology* 1964; 14:222-231.
- Gilson AS, Mills WB. Activities of single motor units in man during slight voluntary efforts. *Am J Physiol* 1943; 133:648-669.
- Gleason TF, Goldstein WM, Ray RD. The function of the anconeus muscle. *Clin Orthop Relat Res* 1985; 192:147-148.
- Harwood B, Choi IH, Rice CL. Reduced motor unit discharge rates of maximal velocity dynamic contractions in response to a submaximal dynamic fatigue protocol. *J Appl Physiol* 2012a; 113(12):1821-1830.

- Harwood B, Dalton BH, Power GA, Rice CL. Motor unit properties from three synergistic muscles during ramp isometric elbow extensions. *Exp Brain Res* 2013; 231(4):501-510.
- Harwood B, Davidson AW, Rice CL. Motor unit discharge rates of the anconeus muscle during high-velocity elbow extensions. *Exp Brain Res* 2011; 208:103-113.
- Harwood B, Rice CL. Changes in motor unit recruitment thresholds of the human anconeus muscle during torque development preceding shortening elbow extensions. *J Neurophysiol* 2012; 107(10):2876-2884.
- Henneman E. Relation between size of neurons and their susceptibility to discharge. *Science* 1957; 126(3287):1345-1347.
- Hwang K, Han JY, Chung IH. Topographical anatomy of the anconeus muscle for use as a free flap. *J Reconstr Microsurg* 2004; 20:631-636.
- Kennett RP and Fawcett PRW. Repetitive nerve stimulation of anconeus in the assessment of neuromuscular transmission disorders. *Electroencephalogr Clin Neurophysiol* 1993; 89:170-176.
- Kwah LK, Pinto RZ, Diong J, Herbert RD. Reliability and validity of ultrasound measurements of muscle fascicle length and pennation in humans: a systematic review. *J Appl Physiol* 2013; 114(6):761-769.
- Liddell EGT, Sherrington CS. Recruitment and some other factors of reflex inhibition. *Proc R Soc Lond* 1925; 1925(B97):488-518.
- Lieber RL, Friden J. Functional and clinical significance of skeletal muscle architecture. *Muscle Nerve* 2000; 23(11): 1647-1666.

- Lieber RL. Skeletal muscle structure and function: implications for physical therapy and sports medicine. Baltimore: Williams & Wilkins, 303.
- Maganaris C, Baltzopoulos V. Predictability of in vivo changes in pennation angle of human tibialis anterior muscle from rest to maximum isometric dorsiflexion. *Eur J Appl Physiol Occup Physiol* 1999; 79:294-297.
- Maselli RA, Mass DP, Distad BJ, Richman DP. Anconeus muscle: a human muscle preparation suitable for in-vitro microelectrode studies. *Muscle Nerve* 1991; 14:1189-1192.
- McComas AJ, Fawcett PR, Campbell MJ, Sica RE. Electrophysiological estimation of the number of motor units within a human muscle. *J Neurol Neurosurg Psychiatry* 1971; 34(2):121-131.
- McNeil CJ, Doherty TJ, Stashuk DW, Rice CL. The effect of contraction intensity on motor unit number estimates of the tibialis anterior. *Clin Neurophysiol* 2005; 116:1342-1347.
- Molinier F, Laffosse JM, Bouali O, Tricoire JL, Moscovici J. The anconeus, an active lateral ligament of the elbow: new anatomical arguments. *Surg Radiol Anat* 2011; 33(7):617-621.
- Pasquet B, Carpentier A, Duchateau J. Change in muscle fascicle length influences the recruitment and discharge rate of motor units during isometric contractions. *J Neurophysiol* 2005; 94(5):3126-3133.
- Pasquet B, Carpentier A, Duchateau J. Specific modulation of motor unit discharge for a similar change in fascicle length during shortening and lengthening contractions in humans. *J Physiol* 2006; 577(2):753-765.

- Pereira BP. Revisiting the anatomy and biomechanics of the anconeus muscle and its role in elbow stability. *Ann Anat* 2013; 195(4):365-370.
- Power GA, Dalton BH, Behm DG, Doherty TJ, Vandervoort AA, Rice CL. Motor unit survival in lifelong runners is muscle dependent. *Med Sci Sports Exerc* 2012; 44(7):1235-1242.
- Power GA, Dalton BH, Behm DG, Vandervoort AA, Doherty TJ, Rice CL. Motor unit number estimates in masters runners: use it or lose it? *Med Sci Sports Exerc* 2010; 42(9):1644-1650.
- Shefner JM. Motor unit number estimation in human neurological diseases and animal models. *Clin Neurophysiol* 2001; 112(6):955-964.
- Simoneau EM, Longo S, Seyennes OR, Narici MV. Human muscle fascicle behaviour in agonist and antagonist isometric contractions. *Muscle Nerve* 2012; 45(1):92-99.
- Stashuk DW. Decomposition and quantitative analysis of clinical electromyographic signals. *Med Eng Phys* 1999; 21(6-7):389-404.
- Travill AA. Electromyographic study of the extensor apparatus of the forearm. *Anat Rec* 1962; 144:373-376.
- Zhang LQ, Nuber GW. Moment distribution among human elbow extensor muscles during isometric and submaximal extension. *J Biomech* 2000; 33:145-154.

2.0 STUDY 1: Muscle Architectural Properties of the Anconeus

2.1 INTRODUCTION

Muscle architecture, together with fiber type composition and distribution, is an important determinant of muscle contractile properties (Edgerton et al., 1975; Lieber and Bodine-Fowler, 1993; Kellis et al., 2012; Gerling et al., 2013). Muscle architecture has been classically studied using cadaver tissue. However, the applicability of measurements obtained from cadavers is limited by the age of the tissue, and can only be described at the angle for which the joint is fixed (Narici et al., 1996; Fukunaga et al., 1997). Alternatively, ultrasonography has facilitated the reliable measure of architectural variables at rest, and during static and dynamic contractions, in many human skeletal muscles *in vivo* (Narici et al., 1996; Fukunaga et al., 1997; Kawakami et al., 1998; Chleboun et al., 2001; Chleboun et al., 2007, Power et al., 2013; Kwah et al., 2013).

One small and seemingly insignificant muscle of the elbow joint, the anconeus, has been used frequently as a model in neuromuscular and anatomical investigations. The anconeus has been shown to provide high-quality recordings of motor unit (MU) properties during isometric and dynamic elbow extensions (Harwood et al., 2011; 2012a; Harwood and Rice, 2012; Stevens et al., 2013), has been used to record surface and intramuscular electromyography (EMG) to study synergistic elbow extensor activity (Le Bozec and Maton, 1982; Davidson and Rice, 2010; Harwood et al., 2013), and is often used clinically in the assessment of neuromuscular transmission disorders (Kennett and Fawcett, 1993; Maselli et al., 1991). One explanation for the high intramuscular signal clarity of anconeus intramuscular EMG recordings over the full range of dynamic elbow extensions (Harwood et al., 2011; 2012a) is that MU number estimates of the anconeus

are relatively low compared to other skeletal muscles, which manifests as less electrical interference from adjacent MUs and a less dense signal (Stevens et al., 2013). An alternative or complementary explanation for the high intramuscular EMG clarity of the anconeus may be that minimal physical displacement of the recording electrode during contractile shortening occurs due to smaller absolute changes in architectural features compared with other skeletal muscles. However, this hypothesis has not been substantiated *in vivo*.

Two architectural features are measured predominantly using ultrasonography: fascicle length (L_F) and pennation angle (PA). Fascicle length, which is an estimate of muscle fiber length, is defined as the length of a line coincident with the fascicle between the deep and superficial aponeuroses. Fascicle length indicates the range of lengths over which the muscle is capable of actively producing force, known as the excursion potential (Lieber and Friden, 2000). Pennation angle represents the angle of the muscle fibers that comprise a muscle fascicle relative to the force-generating axis, and directly affects both the force production and the excursion (Gans and De Vree, 1987); wherein larger angles of pennation limit the excursion potential. It is apparent from ultrasound imaging that these architectural variables are dynamic; changing in response to muscle length changes, or in response to a transition from rest to contraction (including isometric) (Narici et al., 1996; Fukunaga et al., 1997). For example, Chleboun et al. (2001) demonstrated a disordinal interaction between L_F and PA of the human biceps femoris muscle in a relaxed state as a function of hip and knee angles. Similarly in the tibialis anterior, it has been shown that L_F decreases and PA increases at higher isometric dorsiflexion contractile intensities (Maganaris et al, 1999, Simoneau et al., 2012). Alterations in L_F

and PA accommodate the shortening or lengthening of sarcomeres responding to variations in tendon slack and changes in physiological cross-sectional area (PCSA), and therefore have important functional relevance.

Except for one pilot study reported in abstract form (Harwood et al., 2010), the anconeus has not been studied *in vivo* using ultrasonography. Several cadaveric (Pereira, 2013; Ng et al., 2012; Molinier et al., 2011; Coriolano et al., 2009) and EMG (Basmajian et al., 1972; Le Bozec and Maton, 1982; Bergin et al., 2013) studies have described the gross anatomy of the anconeus, and largely defined its function. From these various independent anatomical and functional studies, the primary functions of the anconeus seem to be active stabilization of the elbow joint (Pereira, 2013; Molinier et al., 2011; Kendall et al., 1980), with an approximate 15% contribution to maximum elbow extension torque (Basmajian et al., 1972; Le Bozec and Maton, 1982; Zhang et al., 2000). Despite a description of *in situ* anatomy from cadavers, it is important to understand architectural features *in vivo* as these properties may affect the recruitment and rate coding patterns of individual MUs during various types of contractions (Pasquet et al., 2006; 2005). In addition, it is important to determine the degree to which the anconeus responds architecturally throughout the range of motion (ROM) to substantiate the value of this muscle for study during actively changing elbow joint angles. Thus, the purpose of this study was to evaluate, using ultrasonography, the degree of change in architectural features (L_F and PA) of the anconeus at rest across the full ROM for the elbow joint. It is hypothesized that as elbow joint angle increases to full extension (0° of elbow flexion), L_F and PA of the anconeus muscle will decrease and increase, respectively.

2.2 METHODS

2.2.1 Participants

Ten young adult male participants (25 ± 3 y, 178 ± 7 cm, 77 ± 10 kg) volunteered for the study. Participants were asked to refrain from unaccustomed and strenuous upper limb exercise for one day prior to testing and to not consume caffeine within four hours prior to testing. The participants were recruited from the university population and were considered to be recreationally active but not systematically trained. All participants were free from known neuromuscular or cardiovascular diseases. The study protocol was approved by the local university ethics board and conformed to the Declaration of Helsinki. Informed written consent was obtained prior to testing.

2.2.2 Experimental Protocol

Elbow angle was recorded and ultrasound imaging conducted with the participant seated on a HUMAC NORM dynamometer (CSMi Medical Solutions, Stoughton, MA, USA) (Figure 1A). The non-dominant arm (left arm for all participants) was secured tightly to a custom forearm dynamometer attachment at the wrist and midpoint of the forearm (~12cm proximal to the head of the ulna) using two 5cm wide inelastic Velcro restraints, which aligned the medial epicondyle of the humerus with the rotational axis of the dynamometer. Extraneous movements were minimized using inelastic shoulder and waist restraints. Participants sat in an upright position, such that the inertial weight of the left arm was supported in testing position, with the shoulder flexed at 90° and the forearm in a prone position. Ultrasound recordings were obtained at 135° , 120° , 90° , 45° , and 0° of elbow flexion (elbow joint angle of 0° was considered full extension) (Figure 1B).

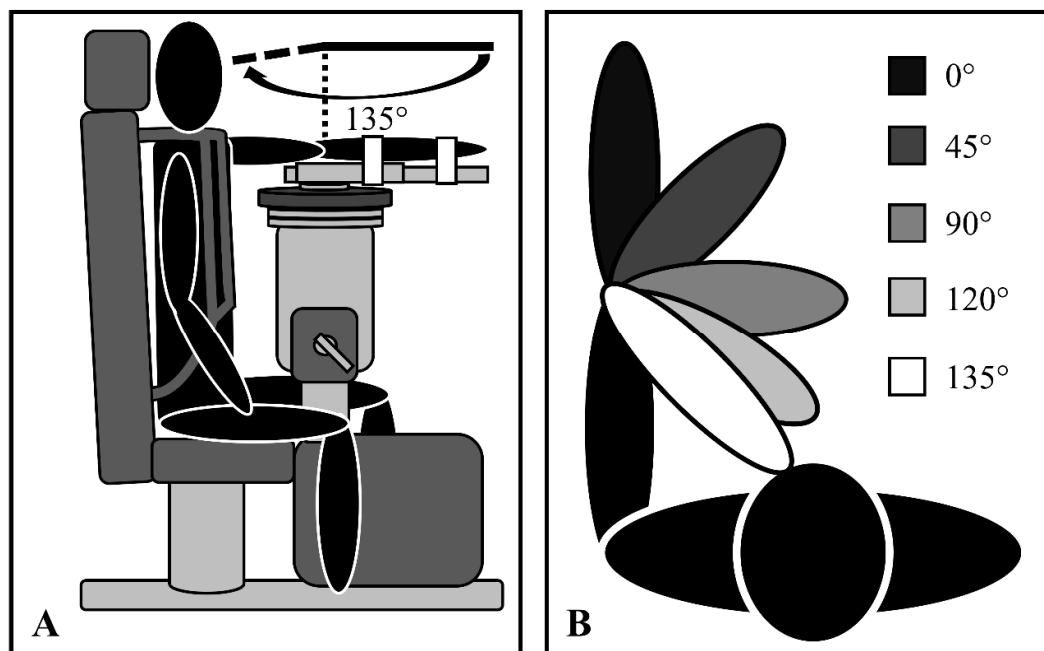


Figure 1. Schematic diagrams of the experimental set up. A) Participant situated in testing position in a HUMAC NORM dynamometer with shoulder flexed at 90° and forearm in prone position (participant shown at 0° elbow flexion). B) Ultrasound imaging positions.

2.2.3 Ultrasonography

To investigate the effect of changing elbow joint angle on L_F and PA, ultrasound imaging was performed using a linear array probe (GE model M12L, 4.9mm, 5-13MHz), attached to a Vivid 7 ultrasound unit (GE Healthcare, Mississauga, Ontario, Canada). Because of the size and location of the muscle in relation to bony contours and fascial sheaths, it was not possible to follow L_F and PA in the anconeus during continuous low intensity contractile movements or at static angles during various contractile intensities. Therefore, images were collected at rest for the five angles of elbow flexion. Briefly, the probe was placed directly on the skin overlying the anconeus muscle approximately 3cm

distal to lateral epicondyle of the humerus, and olecranon process of the ulna. The probe was positioned parallel to the direction of the aponeurosis to allow the fascicles to be displayed as a banded pattern. Once a suitable recording position was obtained (minimum of one distinct muscle fascicles per image (Figure 2A)), the location was marked with indelible ink on the skin surface. Anconeus muscle thickness was determined at 135° and 0° of elbow flexion with the probe positioned perpendicularly to the aponeurosis. The probe was moved distally from the lateral epicondyle of the humerus toward the ulna identifying the deepest border of the anconeus muscle, from which the measurement was made (Figure 2B). Imaging was repeated for a given elbow angle if the operator deemed the previous image unsatisfactory, and was repeated until a useful image was obtained. The probe was held firmly in place by the same operator for all tests and standard ultrasound gel was used as the coupling agent.

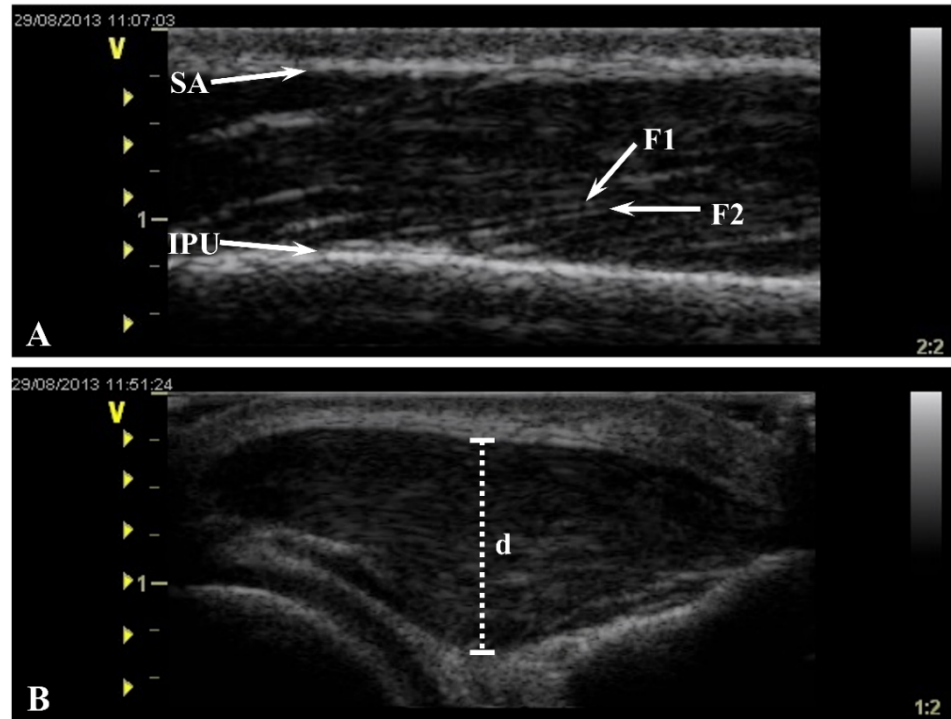


Figure 2. Ultrasound images of the anconeus from a representative participant. A) Longitudinal section visualizing two distinct fascicles (F1 and F2) for 120° of elbow flexion at rest. SA, superficial aponeurosis; IPU, location of fascicle insertion on the posterior face of the ulna. B) Cross section showing muscle thickness measurement (d) for 0° of elbow flexion at rest.

2.2.4 Data Reduction and Analysis

All ultrasound images captured during testing were transferred to a desktop computer for offline analysis using EchoPAC software (v.7.0.1, GE Vingmed Ultrasound, Horton, Norway) which allowed for the calculation of L_F and PA. Pennation angle was defined as the angle created by the fascicle at its insertion point on the posterior face of the ulna. Fascicle length was defined as the length of a line coincident with the fascicle, between the insertion point of the fascicle onto the ulna and the superficial aponeurosis. Images were selected so that fascicles were visible near the point

of insertion onto the ulna. However, the fascicle was often not visible in its entirety, in which case its intercept with the aponeurosis was extrapolated (Reeves and Narici, 2003), as is illustrated in Figure 3.

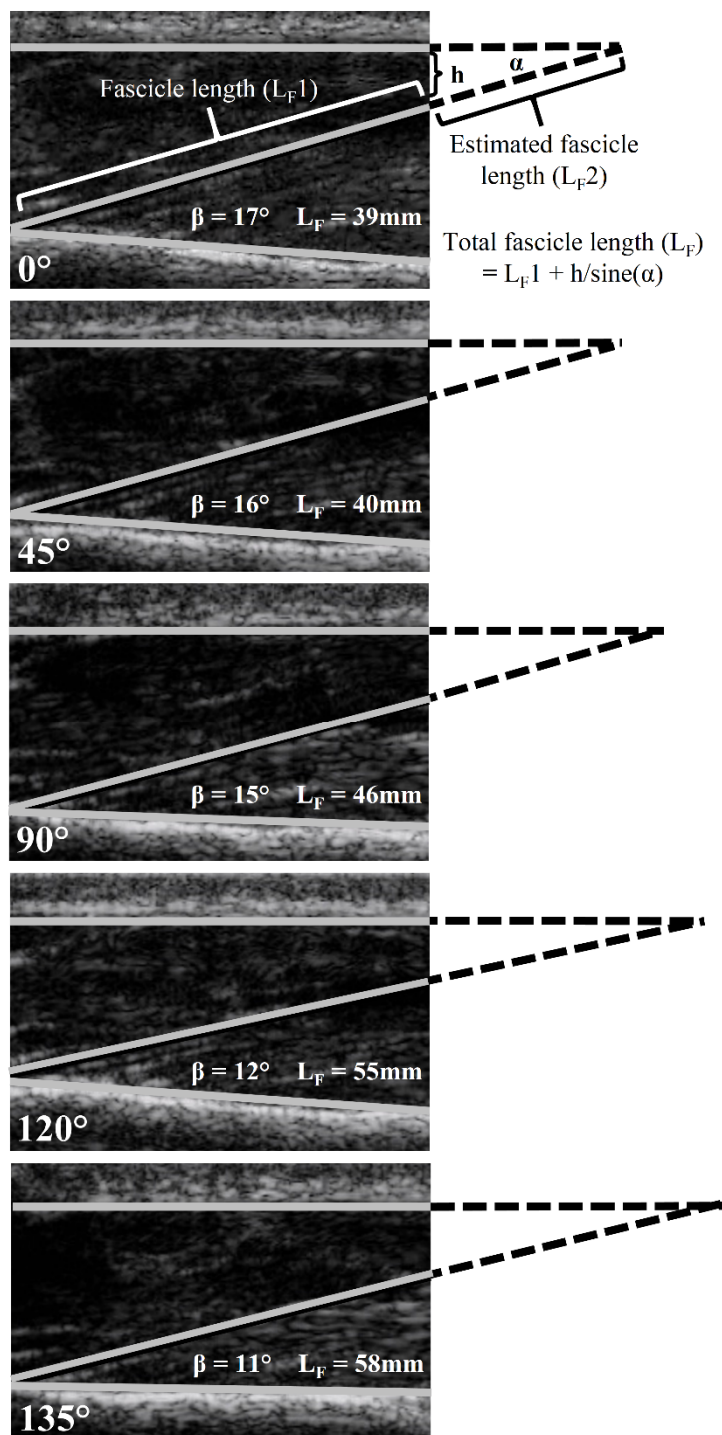


Figure 3. Ultrasound images of the anconeus from a representative participant showing fascicle length (L_F) and pennation angle (PA) measurement at rest. The solid lines represent the aponeurossis and posterior face of the ulna. Pennation angle (denoted as β)

is the angle at which the fascicle leaves the posterior face of the ulna and intersects with the theoretical aponeurosis indicated with an extrapolated broken line. Fascicle length was calculated as the sum of the measured fascicle length (L_{F1}) and the estimated (L_{F2}) fascicle length [$h/\text{Sine}(\alpha)$].

2.2.5 Statistical analysis

Data were analyzed with SPSS statistical software (version 16, SPSS Inc. Chicago, IL). Separate one factor (elbow joint angle) repeated measures univariate analyses of variance (ANOVAs) were performed with an *a priori* repeated contrast, to compare the dependent variables, average L_F and average PA, for each angle of elbow flexion to the subsequent elbow joint angle (135° elbow flexion representing baseline). A paired t-test was used to compare anconeus muscle thickness at 0° and 135° of elbow flexion. The level of significance was set at $P < 0.05$. Data are presented as mean \pm standard deviation (SD).

2.3 RESULTS

Despite the challenges of applying ultrasound to a small muscle that is enveloped by a relatively thick layer of fascia and surrounded by bony contours, useful images were obtained at all joint angles for each participant. On average 3.9 ± 0.5 images were obtained per elbow joint angle, yielding 1.7 ± 0.2 fascicles per participant per elbow joint angle.

In all ten participants, L_F decreased and PA increased from 135-0° of elbow flexion. The overall or maximum change throughout the entire ROM in L_F and PA was 18mm (32%) and 5° (45%), respectively. Average values of L_F decreased by ~12% from 135-120° and 120-90°, and ~11% from 90-45° ($P < 0.05$; Table 1, Figure 4A). Average values of PA were increased from 135-120°, 120-90°, and 45-0° ($P < 0.05$; Table 1, Figure 4B). Percent increase for PA between each elbow joint angle (135-120°, 120-90°, and 45-0°) was determined to be ~12%. The thickness of the muscle ranged from 8-12mm at 135°, and increased by 9% between 135° and 0° of elbow flexion ($P < 0.05$; Table 1).

Table 1. Muscle architecture measurements

Angle of elbow flexion (°)	135	120	90	45	0
Fascicle length (mm)	$56 \pm 7^*$	$50 \pm 9^*$	$44 \pm 9^*$	40 ± 8	38 ± 7
Pennation angle (°)	$11 \pm 1^*$	$12 \pm 2^*$	13 ± 3	$14 \pm 2^*$	16 ± 3
Thickness (mm)	$10 \pm 2^\dagger$	---	---	---	11 ± 2

Measurements were obtained from 10 healthy young males at rest. Values are mean \pm SD.

*denotes a difference compared to the subsequent degree of elbow flexion.

†denotes a difference between 0° and 135° of elbow flexion.

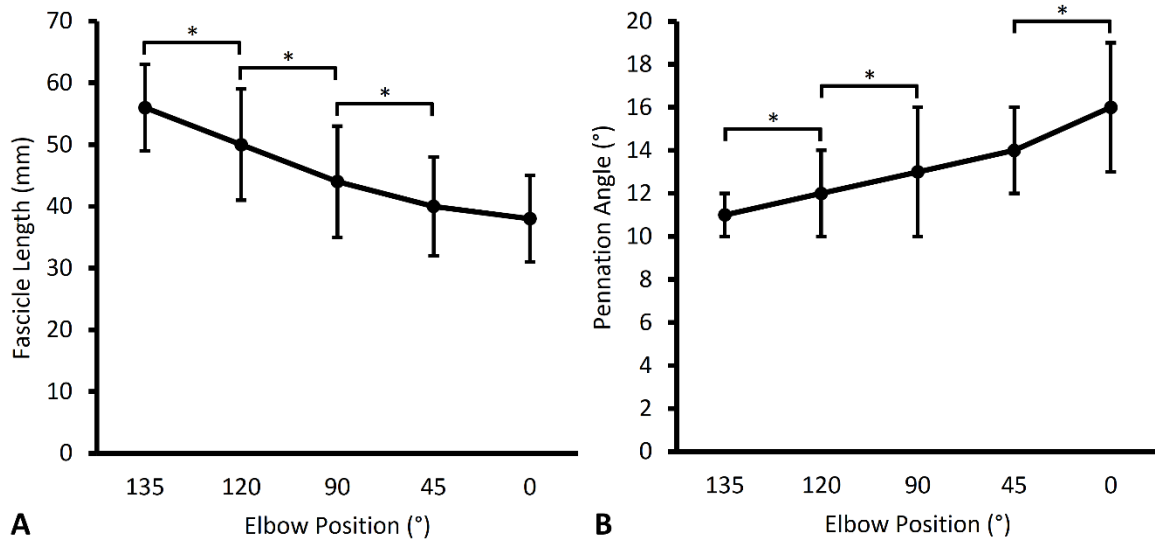


Figure 4. A) Mean fascicle length (mm) at five angles of elbow flexion (°). B) Mean pennation angle (°) at five angles of elbow flexion (°). Data are presented as means \pm SD.

* denotes difference among angles of elbow flexion (P<0.05).

2.4 DISCUSSION

This study examined the architectural features, L_F and PA, of the human anconeus muscle at rest *in vivo* for five elbow joint angles. A few studies have described anconeus muscle architecture from cadavers at a single often unspecified, fixed joint angle (Coriolano et al., 2009; Ng et al., 2012; Pereira, 2013), and one study estimated L_F and PA over a 120° ROM using computer software (Pereira, 2013), but here we investigated these key architectural features using ultrasonography *in vivo* over the full range of elbow joint excursion. The results indicate that anconeus L_F and PA substantially decrease and increase, respectively, as the elbow joint angle approaches full extension from a flexed position. These findings support and extend pilot data tested over a smaller ROM (0-120°) reported in an abstract as relative changes only in L_F and PA (Harwood et al., 2010). Our results have important implications related to neuromuscular function of this muscle as a model for study in health and disease.

Cadaveric studies have described the anatomy of the human anconeus muscle, including muscle architectural measures L_F and PA, yet most do not report a specific elbow joint angle. Average L_F was reported as ~30mm (Coriolano et al., 2009; Pereira, 2013), whereas average PA was determined to be $71 \pm 12^\circ$ (Ng et al., 2012). The moderate discrepancy between the cadaveric L_F value and that reported in the current study (L_F , 46 ± 10 mm), is likely the result of comparing: 1) an average L_F derived from multiple joint angles to a single L_F recorded at one often unspecified angle; and 2) *in vivo* measurements obtained from a healthy, young population to *in situ* preparations from elderly cadavers. Skeletal muscle architecture of human cadaver muscle has been found to differ greatly from age-matched *in vivo* ultrasonographic measurements, wherein

pennation angles and fascicle lengths differed ~13-180% and ~4-21%, respectively, depending on the muscle under investigation (Martin et al., 2001). Martin et al. (2001) attributed these differences to shortened cadaveric fibre bundle length, suggesting that cadaveric muscle exists architecturally in a state of partial contraction. It is likely that this hypothesized state of partial contraction of the muscle partially accounted for the relatively large disparity between cadaveric and *in vivo* values reported here (PA: $13 \pm 3^\circ$), as PAs have been shown to increase relative to muscle length during shortening contractions (Narici et al., 1996; Fukunaga et al., 1997; Kawakami et al., 1993; Maganaris et al., 1999, Simoneau et al., 2012). However, the measurement procedure may have contributed also to the differences between one cadaveric study (Ng et al., 2012) and the present study. In cadavers, the average PA was determined as the angle at which the fascicle intersects 90 degree quarterly intervals along the long axis of the muscle (see Ng et al., 2012, Figure 3). Whereas in the present study, PA was measured as the angle at which the fascicle emerges from its insertion on the posterior face of the ulna. It has been shown that PAs are systematically smaller at the insertion of the muscle onto the tendon compared with those imaged from more central locations of the muscle (Blazevich et al., 2006). Furthermore, anconeus compartmentalization could also explain variations in PA findings (Bergin et al., 2013). Therefore, PA values from the current study may not compare to those extracted from the cadaver study as they represent two related, but distinct, measures.

More important to the purpose of the present study is that the anconeus studies cited above, only described the muscle architecture at a single elbow joint angle (position of fixation). One study (Pereira, 2013) attempted to measure changes in anconeus muscle

fiber length over multiple elbow joint angles (ranging from 0-120° of elbow flexion) using a 2-D kinematic model. That study reported that muscle fiber lengths differed over the ROM tested, with the greatest change recorded at 90° elbow flexion. However, the investigation was limited by a small sample of human cadavers (comprised of eight elderly men) and a simple 2-D kinematic model, which the authors admitted did not fully represent physiological *in vivo* conditions. Thus, the use of ultrasonography was necessary to obtain a more accurate representation of changes in L_F and PA *in vivo* in relation to elbow joint angle. As noted in the introduction, rate coding and MU recruitment patterns are affected by the compliance of the muscle-tendon complex, which is dependent upon changes in muscle architectural properties (Pasquet et al., 2005). Therefore, the ability to investigate the degree of change in L_F and PA *in vivo* is necessary for description of both the anatomy and MU function of the anconeus.

The relative change in L_F and PA reported for the anconeus in the current study closely resembles that derived using ultrasonography for other muscles *in vivo*, under passive conditions, relative to the ROM tested at their respective joints. For example, L_F and PA measured in the biceps femoris at three knee angles, covering a 90° ROM (0°, 45°, 90° flexion), were reported to decrease 27% and increase 27%, respectively (Chleboun et al., 2001). Similarly, in the vastus lateralis, L_F decreased 27% and PA increased 29%, when knee angle changed from 110-0° of flexion (Fukunaga et al., 1997). Moreover, Kawakami et al. (1998) measured percent change in L_F and PA in the relaxed medial gastrocnemius (MG), lateral gastrocnemius (LG), and soleus (SOL) across an ankle joint ROM of 45° (-15-30° extension) and observed a 21%, 23%, and 30% decrease in L_F were reported for the MG, LG, and SOL, respectively, while PA increased 32%,

42%, and 47% in these same muscles. In another study on the MG, Narici et al. (1996) measured L_F and PA changes over a slightly larger ROM (60°), and observed a 40% decrease in L_F and 75% increase in PA. With the exception of the change in PA reported for this MG study (Narici et al., 1996), the percent changes in these muscle groups across a full or nearly full ROM and those reported here for the anconeus (L_F , decreased 32%; PA, increased 45%) are uniform. Thus, although the anconeus is a short stabilizing muscle it does undergo architectural changes during extension as the elbow joint moves throughout a large ROM. Absolute values of PA reported previously for the three heads of the triceps brachii (TB) are also similar to those determined for the anconeus in the present study. Although resting L_F and PA values for the three heads of the TB across the full ROM have not been assessed, different studies have examined their muscle architecture (PA) at different elbow joint angles. Using ultrasound, Blazeovich et al. (2001) found PA for the relaxed lateral head of the TB, in men of similar age as those in the present study, to be $12 \pm 1.8^\circ$ when the elbow was flexed 90° . At 0° of elbow flexion, PAs of $15 \pm 6^\circ$ (Kawakami et al., 1993) and $19.7 \pm 2.9^\circ$ (Kubo et al., 2003) were reported for the TB long head, while $11 \pm 5^\circ$ was observed for the medial head (Kawakami et al., 1993). As mentioned, these values are consistent with those reported in the present study ($13 \pm 3^\circ$ and $16 \pm 3^\circ$ at 90° and 0° of elbow flexion, respectively), indicating anconeus participates in elbow extension movements (Basmajian et al., 1972) and shares similar relative muscle architecture and relative changes in architecture as the TB with elbow excursion, at least with respect to PA.

In summary, L_F and PA of the relaxed anconeus were observed to change as a function of elbow joint angle. The values obtained here, using ultrasonography, differed

slightly to those reported previously in cadaveric studies (Coriolano et al., 2009; Pereira, 2013; Molinier et al., 2011; Ng et al., 2012) with respect to L_F , but were significantly different for PA, which was attributed partially to a difference in measurement procedure and the limitation of comparing *in vivo* measures to cadaveric. Relative change in L_F and PA for the anconeus was consistent with that of other muscles measured using the same technique (Chleboun et al., 2001; Kawakami et al., 1998; Fukunaga et al., 1997). Moreover, absolute values of PA observed for the anconeus were very similar to those reported in the TB (Kubo et al., 2003; Blazevich et al., 2001; Kawakami et al., 1993), which share innervation and function with the anconeus. These similarities in muscle architecture changes indicate that the anconeus behaves like other skeletal limb muscles. Therefore, the high intramuscular EMG signal clarity reported for this muscle during functional contractions does not appear to be related to any unusual architectural feature, supporting the muscle as a valuable model of study in neuromuscular physiology and functional anatomy.

2.5 REFERENCES

- Basmajian JV, Griffin WR. Function of anconeus muscle. An electromyographic study. *J Bone Joint Surg Am* 1972; 54:1712-1714.
- Bergin MJ, Vicenzino B, Hodges, PW. Functional differences between anatomical regions of the anconeus muscle in humans. *J Electromyogr Kinesiol* 2013; 23(6):1391-1397.
- Blazevich AJ, Gill ND, Zhou S. Intra- and intermuscular variation in human quadriceps femoris architecture assessed in vivo. *J Anat* 2006; 209(3):289-310.
- Blazevich AJ, Giorgi A. Effect of testosterone administration and eight training on muscle architecture. *Med Sci Sports Exerc* 2001; 33(1):1688-1693.
- Chleboun GS, Busic AB, Graham KK, Stuckey HA. Fascicle length change of the human tibialis anterior and vastus lateralis during walking. *J Orthop Sports Phys Ther* 2007; 37(7):372-379.
- Chleboun GS, France AR, Crill MT, Braddock HK, Howell JN. In vivo measurement of fascicle length and pennation angle of the human biceps femoris muscle. *Cells Tissues Organs* 2001; 169(4):401-409.
- Coriolano MGWS, Lins OG, Amorim MJAAL, Amorim AA. Anatomy and functional architecture of the anconeus muscle. *Int J Morph* 2009; 27(4):1009-1012.
- Davidson AW, Rice CL. Effect of shoulder angle on the activation pattern of the elbow extensors during a submaximal isometric fatiguing contraction. *Muscle Nerve* 2010; 42(4):514-521.
- Edgerton V, Smith J, Simpson D. Muscle fiber type populations of human leg muscles. *J Histochem Cytochem* 1975; 7:259-266.

- Fukunaga T, Ichinose Y, Ito M, Kawakami Y, Fukashiro S. Determination of fascicle length and pennation in a contracting human muscle in vivo. *J Appl Physiol* 1997; 82(1):354-358.
- Gans C, de Vree F. Functional bases of fiber length and angulation in muscle. *J Morphol* 1987; 192(1):63-85.
- Gerling ME, Brown SH. Architectural analysis and predicted functional capability of the human latissimus dorsi muscle. *J Anat* 2013; 223(2):112-122.
- Harwood B, Choi IH, Rice CL. Reduced motor unit discharge rates of maximal velocity dynamic contractions in response to a submaximal dynamic fatigue protocol. *J Appl Physiol* 2012a; 113(12):1821-1830.
- Harwood B, Dalton BH, Power GA, Rice CL. Motor unit properties from three synergistic muscles during ramp isometric elbow extensions. *Exp Brain Res* 2013; 231(4):501-510.
- Harwood B, Davidson AW, Rice CL. Motor unit discharge rates of the anconeus muscle during high-velocity elbow extensions. *Exp Brain Res* 2011; 208:103-113.
- Harwood B, Hamberg CM, Chleboun GS, Rice CL. Effect of elbow joint angle on anconeus fascicle length and motor unit firing rates. *Med Sci Sports Exerc* 2010; 42(5):584-585.
- Harwood B, Rice CL. Changes in motor unit recruitment thresholds of the human anconeus muscle during torque development preceding shortening elbow extensions. *J Neurophysiol* 2012; 107(10):2876-2884.
- Kawakami Y, Abe T, Fukunaga T. Muscle-fiber pennation angles are greater in hypertrophied than in normal muscles. *J Appl Physiol* 1993; 74(6):2740-2744.

- Kawakami Y, Ichinose Y, Fukunaga T. Architectural and functional features of human triceps surae muscles during contraction. *J Appl Physiol* 1998; 85(2):398-404.
- Kellis E, Galanis N, Kapetanios G, Natsis K. Architectural difference between the hamstring muscles. *J Electromyogr Kinesiol* 2012; 22(4):520-526.
- Kennett RP, Fawcett PR. Repetitive nerve stimulation of anconeus in the assessment of neuromuscular transmission disorders. *Electroencephalogr Clin Neurophysiol* 1993; 89(3):170-176.
- Kubo K, Kanehisa H, Azuma K, Ishizu M, Kuno SY, Okada M, Fukunaga T. Muscle architectural characteristics in young and elderly men and women. *Int J Sports Med* 2003; 24(2):125-130.
- Kwah LK, Pinto RZ, Diong J, Herbert RD. Reliability and validity of ultrasound measurements of muscle fascicle length and pennation in humans: a systematic review. *J Appl Physiol* 2013; 114(6):761-769.
- Le Bozec S, Maton B. The activity of anconeus during voluntary elbow extension: the effect of lidocaine blocking of the muscle. *Electromyogr Clin Neurophysiol* 1982; 22(4):265-75.
- Lieber RL, Bodine-Fowler SC. Skeletal muscle mechanics: implications for rehabilitation. *Phys Ther* 1993; 73(12):844-856.
- Lieber RL, Friden J. Functional and clinical significance of skeletal muscle architecture. *Muscle Nerve* 2000; 23(11): 1647-1666.
- Maganaris C, Baltzopoulos V. Predictability of in vivo changes in pennation angle of human tibialis anterior muscle from rest to maximum isometric dorsiflexion. *Eur J Appl Physiol Occup Physiol* 1999; 79:294-297.

Martin DC, Medri MK, Chow RS, Oxoron V, Leekam RN, Agur AM, McKee NH.

Comparing human skeletal muscle architectural parameters of cadavers with in vivo ultrasonographic measurements. *J Anat* 2001; 199(pt. 4): 429-434.

Maselli RA, Mass DP, Distad BJ, Richman DP. Anconeus muscle: a human muscle preparation suitable for in-vitro microelectrode studies. *Muscle Nerve* 1991; 14:1189-1192.

Molinier F, Laffosse JM, Bouali O, Tricoire JL, Moscovici J. The anconeus, an active lateral ligament of the elbow: new anatomical arguments. *Surg Radiol Anat* 2011; 33(7):617-621.

Narici MV, Binzoni T, Hiltbrand E, Fasel J, Terrier F, Cerretelli P. In vivo human gastrocnemius architecture with changing joint angle at rest and during graded isometric contraction. *J Physiol* 1996; 496:287-297.

Ng ZY, Lee SW, Mitchell JH, Fogg QA, Hart AM. Functional anconeus free flap for thenar reconstruction: a cadaveric study. *Hand* 2012; 7(3):286-292.

Pasquet B, Carpentier A, Duchateau J. Change in muscle fascicle length influences the recruitment and discharge rate of motor units during isometric contractions. *J Neurophysiol* 2005; 94(5):3126-3133.

Pasquet B, Carpentier A, Duchateau J. Specific modulation of motor unit discharge for a similar change in fascicle length during shortening and lengthening contractions in humans. *J Physiol* 2006; 577(2):753-765.

Pereira BP. Revisiting the anatomy and biomechanics of the anconeus muscle and its role in elbow stability. *Ann Anat* 2013; 195(4):365-370.

- Power GA, Makrakos DP, Rice CL, Vandervoort AA. Enhanced force production in old age is not a far stretch: an investigation of residual force enhancement and muscle architecture. *Physiol Rep* 2013; 1(1):e00004.
- Reeves ND, Narici MV. Behaviour of human muscle fascicles during shortening and lengthening contractions in vivo. *J Appl Physiol* 2003; 95(3):1090-1096.
- Simoneau EM, Longo S, Seyennes OR, Narici MV. Human muscle fascicle behaviour in agonist and antagonist isometric contractions. *Muscle Nerve* 2012; 45(1):92-99.
- Stevens DE, Harwood B, Power GA, Doherty TJ, Rice CL. Anconeus motor unit number estimates using decomposition-based quantitative electromyography. *Muscle Nerve* 2013. doi: 10.1002/mus.24092.
- Zhang LQ, Nuber GW. Moment distribution among human elbow extensor muscles during isometric and submaximal extension. *J Biomech* 2000; 33:145-154.

3.0 STUDY 2: Motor Unit Number Estimation of the Anconeus¹

3.1 INTRODUCTION

The ability to objectively assess the number of functioning motor units (MUs) in human muscle has important implications for the study of health (Sorenson et al., 2006; Daube et al., 2009), adult aging (Power et al., 2012; McNeil et al., 2005; Dalton et al., 2008), and diseases of lower motoneurons (Bromberg et al., 2008; Olney et al., 2000). Many methods have been used to derive a MU number estimate (MUNE) (Bromberg, 2007), one of which includes decomposition-enhanced spike-triggered averaging (DE-STA) (Stashuk et al., 2003). Decomposition-enhanced spike-triggered averaging has proven to be a reliable and valid technique for estimating the number of MUs in a muscle group (Doherty et al., 2009; Boe et al., 2004; 2006). However, DE-STA can be affected by muscle activation level and contractile force (McNeil et al., 2005; Dalton et al., 2008; Stashuk et al., 2003; Boe et al., 2004). In even a simple task, the resultant net force produced is a combination of multiple forces contributed by usually more than one muscle acting synergistically. Therefore, the many individual force-electromyography (EMG) relationships of the various contributing muscles form the resultant force-EMG relationship for the whole muscle complex. An example of this disproportionate

¹A version of this chapter has been published. Used with permission from *John Wiley and Sons*.

Stevens DE, Harwood B, Power GA, Doherty TJ, Rice CL. Anconeus motor unit number estimates using decomposition-based quantitative electromyography. *Muscle Nerve* 2013; doi: 10.1002/mus.24092

contribution to resultant force is the human elbow extensors, which are comprised of the three heads of the triceps brachii (medial, long, and lateral) and the anconeus. The three heads of the triceps brachii contribute ~85% of the resultant elbow extension torque, whereas the small (cross-sectional area = 2,002mm²), primarily type I (60-67%) anconeus muscle, which acts both to extend the elbow and abduct the ulna during resisted pronation (Travill, 1962; Basmajian and Griffin, 1972; Le Bozec and Maton, 1982; Hwang et al., 2004), contributes less than ~15% to maximal elbow extension torque (Zhang and Nuber, 2000). Furthermore, the relative contribution to force of any single component of the elbow extensors is affected by shoulder joint angles (Davidson and Rice, 2010).

Despite the relative small size of the anconeus it is considered a very useful clinical model in investigation of radial nerve function (Gassel and Diamantopoulos, 1964), neuromuscular transmission *in vitro* (Maselli et al., 1991), myasthenia gravis, Lambert-Eaton myasthenic syndrome, and congenital myasthenic syndromes (Kennett and Fawcett, 1993). In non-clinical models, the anconeus has been shown to be valuable in the study of MU properties during static and dynamic elbow extension contractions, and during fatiguing tasks (Harwood et al., 2011; 2012a; 2012b). The anconeus is easily accessible for needle EMG recordings and compared with other limb muscles (Pasquet et al., 2006; Abellaneda et al., 2009), MU recordings exhibit high signal-to-noise ratios across a broad range of elbow extension torque and contractile velocities (Harwood et al., 2011; 2012a; 2012b), and are active throughout all contraction intensities (Harwood et al., 2012b). These properties indicate the anconeus is an attractive model for decomposition-based quantitative EMG (DQEMG) techniques used in MUNE studies,

because a greater signal-to-noise ratio allows for a better quality and yield of surface-detected individual motor unit potentials (S-MUPs), especially at higher levels of muscle activation. Despite the clinical and practical utility of this muscle for studying MU properties, and the many muscle architectural investigations (Hwang et al., 2004; Pereira, 2013; Coriolano et al., 2007, Naito et al., 1991), the functional anatomy of the anconeus is not understood completely. Furthermore, whether the relatively less complex interference pattern of anconeus intramuscular EMG recordings may be due to a low number of MUs in the muscle has not yet been explored.

In order to provide a comprehensive assessment of the number of functional MUs with DE-STA, the contraction intensity should equal or exceed the upper limit of MU recruitment, such that all MUs, or at least a large proportion of the MU pool (low and high threshold MUs), are active and contributing to the mean S-MUP amplitude. A limitation of most muscles studied to date using the DE-STA MUNE technique is the inability to discriminate S-MUPs of active MUs at forces higher than ~30% of maximum voluntary contraction (MVC) (Doherty and Stashuk, 2003). It is known that the anconeus nears MU recruitment completion at ~25-35%MVC during an isometric contraction (Harwood et al., 2012b). Accordingly, this study estimated the number of functional MUs in the anconeus, using DE-STA, at low (10%), moderate (30%), and higher (50%) relative muscle activation levels (root-mean-square of MVC (RMS_{MVC})), to determine the effect of varying levels of muscle activation on MUNE in healthy, young men. We hypothesized that at higher levels of muscle activation (i.e., 50% RMS_{MVC}), a representative portion of the entire anconeus MU pool would be sampled, resulting in lower MUNE compared with those estimated at lower activation levels.

3.2 METHODS

3.2.1 Participants

Ten young men (25 ± 3 y, 178 ± 7 cm, 77 ± 10 kg) participated in this study. The participants were recruited from the university population and were considered to be recreationally active and not systematically trained. All participants were free from known neuromuscular or cardiovascular diseases. The study protocol was approved by the local University ethics board and conformed to the Declaration of Helsinki. Informed written consent was obtained prior to testing.

3.2.2 Experimental Protocol

Participants were asked to refrain from strenuous exercise one day prior to testing and to not consume caffeine on the day of testing. Elbow extension force was recorded using a custom isometric dynamometer constructed so that the weight of the left upper limb (non-dominant in all subjects) was supported in the testing position with the shoulder and elbow flexed 90° , and the forearm in the prone position. A Velcro strap secured the wrist to a padded, convex, plastic cup (5x10cm) attached to the strain gauge (Model SST-700-100A; ASTechnology, Halliburton, Ontario, Canada) (Figure 5A). Participants' backs were stabilized firmly to eliminate extraneous body movements and posterior displacement of the shoulder during elbow extension.

Data collection began with determination of the maximal compound muscle action potential (CMAP) of the anconeus (Figure 5B). A stimulating bar electrode was held firmly over the radial nerve ~10cm proximal to the olecranon process on the lateral aspect of the arm, and current was increased until the CMAP was achieved. The active electrode was repositioned to minimize the visible rise time of the CMAP negative-peak

amplitude, ensuring the recording electrode was over the motor point. Surface-detected and intramuscular EMG of the anconeus were acquired using DE-STA software on a Neuroscan Comperio system (Neurosoft, El Paso, Texas). One pair of self-adhering Ag-AgCl electrodes (1x1.5cm; Marquette Medical Systems, Jupiter, Florida) was placed over the midpoint of the anconeus muscle belly in a monopolar configuration with an active electrode ~2-4cm distal to the space between the olecranon process of the ulna and the lateral epicondyle of the humerus, and the reference electrode ~10cm distal to the olecranon process of the ulna (Coriolano et al., 2007). To record neuromuscular properties of the lateral and long heads of the triceps brachii and short head of the biceps brachii, pairs of self-adhering pediatric cloth electrodes (2.25x3.5cm; Tyco Healthcare Group Ltd, Mansfield, Massachusetts) were positioned over the posteromedial surface of the left arm in a bipolar configuration: (1) over the long head of the triceps brachii ~10-15cm distal to the axilla; (2) over the posterolateral surface of the left arm ~20cm proximal to the lateral epicondyle of the humerus; and (3) over the anteromedial surface of the arm ~20cm proximal to the medial epicondyle of the humerus for the short head of the biceps brachii. All electrode pairs were positioned at an inter-electrode distance of 2cm. To reduce impedance at the skin-electrode interface, electrode placement was preceded by cleaning the skin with an alcohol-based tissue pad. Intramuscular EMG was recorded via a disposable concentric needle electrode with a recording surface of 0.03mm^2 (Model N53153; Teca, Hawthorne, New York) inserted into the anconeus 6-8mm distal to the active surface electrode (Figure 5A).

Following determination of the anconeus CMAP, single pulse percutaneous muscle stimulation of elbow extensors was delivered using a constant voltage (pulse

width 100 μ s) stimulator (DS7AH; Digitimer, Ltd., Welwyn Garden City, Hertfordshire, UK) to elicit a mechanical twitch. Two custom-made aluminum foil stimulation pads (ranging from 5x6cm to 5x12cm depending on arm size) were coated in electrode gel and firmly secured transversely over the muscle belly of the triceps brachii with the anode positioned ~10cm proximal to the olecranon process of the ulna and the cathode ~10cm distal to the axilla. Visual inspection and palpation was used to ensure that only the elbow extensors, including the anconeus, were activated during electrical stimulation. Finally, current intensity of the stimulator (45-95mA) was increased until no additional twitch force was generated and then increased by 15% to ensure supramaximal stimulation.

Participants then performed a series of MVCs, of which the RMS amplitude of EMG at the greatest force (RMS_{MVC}) was used to establish the 10%, 30%, and 50% target RMS_{MVC} . Another MVC was then performed with electrical stimulation to assess voluntary activation, using the interpolated twitch technique (Belanger and McComas, 1981), and measure neuromuscular properties of the elbow extensors. All MVCs lasted 3-5s, were separated by at least 3min rest, and did not exceed 3-4 contractions in total. Participants were encouraged verbally, and visual feedback of force was provided on a 22" LED computer monitor positioned directly in front of them at a distance of ~1.8m. A subsequent MVC was performed during which EMG of the anconeus, long and lateral heads of the triceps brachii, and short head of the biceps brachii were recorded without electrical stimulation to establish a baseline of surface EMG activity for each muscle. Prior to beginning submaximal targeting contractions, a maximal (3s) voluntary effort (MVE) of the elbow flexors against experimenter resistance was performed to establish

the maximal EMG of the short head of the biceps brachii. The concentric needle electrode was then inserted into the anconeus distal to the active recording electrode, and participants were asked to match a target line of 10%, 30%, or 50% RMS_{MVC} of the muscle in a randomized order. The investigator manipulated the concentric needle to minimize rise times of the negative-peak amplitudes of the first 2-3 detected MU potentials (MUPs). Needle repositioning was completed by either adjusting the depth of insertion or sampling from a new area. Participants were then asked to gradually increase elbow extension force to the %RMS target line within 1-2s and hold the contraction steady for 30s, during which time both the intramuscular EMG of the anconeus and surface-detected EMG of all four muscle groups were obtained simultaneously and stored for further analysis. Participants were given at least 1min of rest between submaximal contractions. Targeting contractions were performed in a random order until at least 20 suitable MUP trains and their respective S-MUPs were sampled for each %RMS target amplitude (Boe et al., 2009) (Figure 5B). Following the protocol, a single elbow extensor MVC was performed to ensure there was no fatigue as a result of the contractions.

Intramuscular EMG signals were band-pass filtered from 10Hz-10kHz and digitized and stored using the Neuroscan Comperio system (Neuroscan Medical Systems, El Paso, TX). Surface EMG signals of the lateral and long heads of the triceps brachii, and the short head of the biceps brachii were pre-amplified (x100), amplified (x2), band-pass filtered (10-1,000Hz) (Neurolog, Welwyn City, UK) and sampled at 2500Hz using a Power 1401 (Cambridge Electronic Design, Cambridge, UK) for offline analysis. Lastly, force data were analog-to-digital converted at a rate of 1000Hz (Power 1401, Cambridge Electronic Design, Cambridge, UK) for offline analysis.

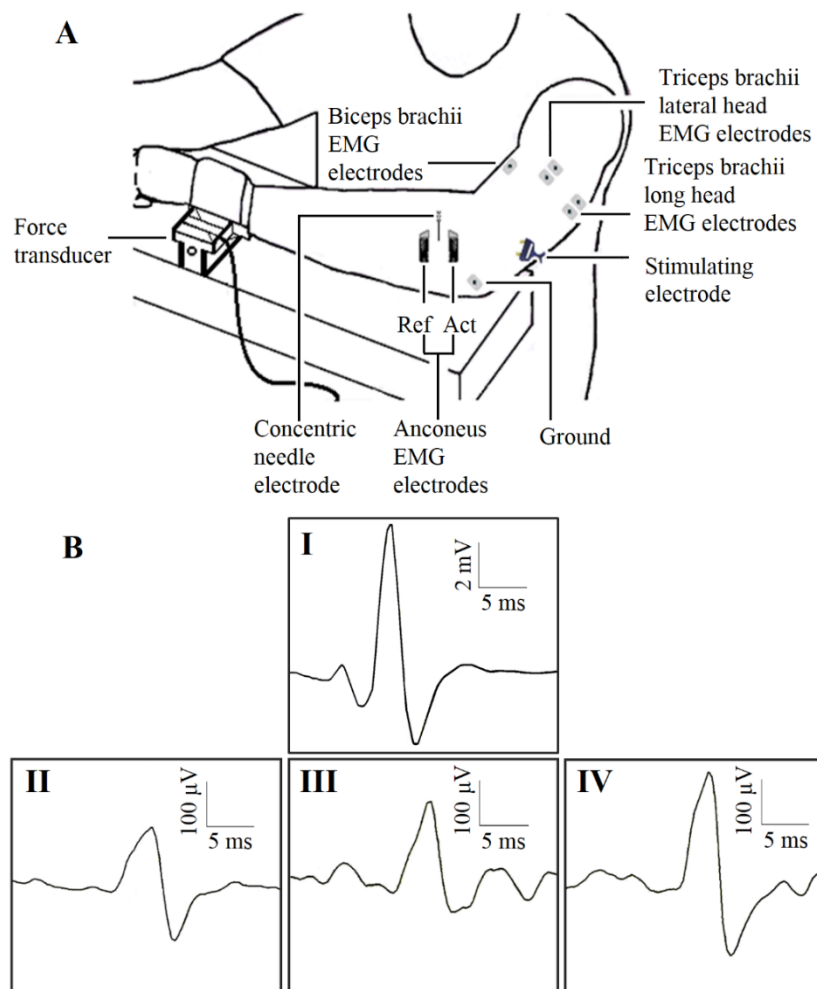


Figure 5. A) Depiction of a participant situated in testing position in a custom dynamometer with shoulder and elbow flexed 90° and forearm in prone position. Pediatric cloth electrodes for the biceps brachii (partially shown in image) and the lateral and long heads of the triceps brachii are shown. Reference (Ref) and active (Act) Ag-AgCl electrodes are shown over the anconeus. A concentric needle electrode is shown inserted into the anconeus (~5-10mm distal to Act electrode), and the stimulating electrode is depicted over the radial nerve (~10cm proximal to olecranon process). (B) Raw EMG tracings from a representative participant. (I) Electrically evoked CMAP and

voluntarily generated mean S-MUP at: (II) $10\%RMS_{MVC}$, (III) $30\%RMS_{MVC}$, and (IV) $50\%RMS_{MVC}$.

3.2.3 Data Reduction and Analysis

Spike2 (version 7.10) software (CED, Cambridge, UK) was used for all off-line analyses. A custom-designed script was used to determine the force of each MVC and target contraction, coefficient of variation (CV) of target contractions, and evoked twitch forces and twitch contraction durations (time-to-peak twitch force + half-relaxation time). The peak RMS value of the surface-detected EMG signal of the elbow extensors was calculated for the MVC during a 1s period at the peak plateau in force amplitude of the MVC. Similarly, MVE of the biceps brachii was expressed by determining the RMS of the MVE (RMS_{MVE}), however, RMS_{MVE} was calculated over a 1s period at the midpoint of the contraction in the absence of an elbow flexion force recording. Average RMS_{MVC} of the lateral and long heads of the triceps brachii, and RMS_{MVE} of the short head of the biceps brachii were determined for the 30s period of each target contraction in which the percent RMS_{MVC} of the anconeus was relatively constant. All RMS values were expressed relative to either the RMS_{MVC} (elbow extensors) of their respective muscle, or the RMS_{MVE} (short head of the biceps brachii).

All off-line analyses of DE-STA MUNE_s were completed by the same experienced operator using previously defined criteria (Boe et al., 2009). Decomposed EMG signals were reviewed off-line to ensure the accuracy of the automated decomposition procedure. Motor unit potential trains with at least 50 detected discharges were required and acted as triggers for spike-triggered averaging of the surface EMG signal. The MU discharge pattern was then inspected visually for a stable and

physiological rate of ~12Hz (i.e., $CV \leq 30\%$) (Harwood et al., 2011). The interspike interval histogram was examined to confirm a Gaussian distribution. Motor unit potential trains that did not meet these criteria were excluded from further analysis. Next, S-MUPs were inspected to identify a distinct waveform which was temporally linked to the needle potential (within 10ms). The computer generated negative-peak onset and negative-peak amplitude markers of the acceptable S-MUPs were inspected and repositioned manually if necessary to ensure they were accurate with respect to the waveform characteristics they represented (Boe et al., 2006; 2009). A computer algorithm automatically aligned the negative onset markers for all accepted S-MUPs and generated a mean S-MUP template based upon their data-point by data-point average (Doherty and Stashuk, 2003). Finally, a MUNE was derived by dividing the negative-peak amplitude of the CMAP by the negative-peak amplitude of the mean S-MUP.

3.2.4 Statistical Analysis

Data were analyzed with SPSS (version 16, Chicago, Illinois). For S-MUPs, frequency distribution histograms were generated at each relative muscle activation level ($\%RMS_{MVC}$). A repeated measures univariate analysis of variance (ANOVA) was performed to identify differences between contractile levels for all EMG and force measures. When a main effect was observed, a Tukey's HSD *post hoc* analysis was performed with a modified Bonferroni correction factor to determine where significant differences existed among contraction intensities. Linear regression analyses (R^2) were performed to evaluate the shared variance between elbow extension force ($\%MVC$) and EMG amplitude ($\%RMS_{MVC}$) for all four muscles investigated. The alpha level was set

at $P \leq 0.05$. Graphical and tabular data are presented as means \pm SE and means \pm SD, respectively.

3.3 RESULTS

The average elbow extension MVC, twitch amplitude, and twitch contraction duration of the participants in this study were 228.8 ± 79.1 N, 22.1 ± 8.8 N, and 145.4 ± 19.9 ms, respectively. Voluntary activation was near maximal in all participants ($98.9 \pm 0.9\%$). The distributions of S-MUP negative-peak amplitudes were different for the three levels of activation, with $50\%RMS_{MVC}$ yielding the most inclusive range (Figure 6). Compared with average S-MUP negative-peak amplitudes at $10\%RMS_{MVC}$, average anconeus S-MUP negative-peak amplitude were $\sim 30\%$ and $\sim 57\%$ greater at 30% and $50\%RMS_{MVC}$, respectively, and $50\%RMS_{MVC}$ was 38% greater compared with $30\%RMS_{MVC}$ ($P < 0.05$, Figure 7A). Accordingly, anconeus MUNE were less with each increase in target EMG amplitude ($P < 0.05$, Figure 7B).

Average relative elbow extension forces ($\%MVC$) were consistently below the relative target EMG amplitude ($\%RMS_{MVC}$) of the anconeus, but the difference was less with each increase in target EMG amplitude (Figure 8A). Relative EMG amplitudes ($\%RMS_{MVC}$) of the lateral and long heads of the triceps brachii and the short head of the biceps brachii increased with the relative target EMG amplitudes of the anconeus (Figure 8B) and elbow extension force ($\%MVC$) (Figure 8A). Antagonist coactivation of the biceps brachii was $\sim 12\%$ across all target EMG amplitudes of the anconeus ($P < 0.05$, Figure 8A). However, the difference between the EMG amplitude of the anconeus compared with the lateral head and the long head of the triceps brachii decreased with increasing target EMG amplitudes of the anconeus ($\sim 45\%$ at $30\text{-}50\%RMS_{MVC}$ vs. $\sim 80\%$ at $10\%RMS_{MVC}$, $P < 0.05$, Figure 8B).

Table 2. Compound muscle action potential of the anconeus and contractile properties of the elbow extensors

Group	CMAP (mV)	MVC (N)	Pt (N)	PPt (N)	VA (%)	Post MVC (N)
n=10	5.5±1.8	230.4±74.2	28.9±12.2	41.9±14.8	98.9±0.9	236.2±72.2

Values are mean ± SD. CMAP, compound muscle action potential; MVC, maximal voluntary contraction; Pt, resting twitch; PPt, potentiated twitch; VA, voluntary activation.

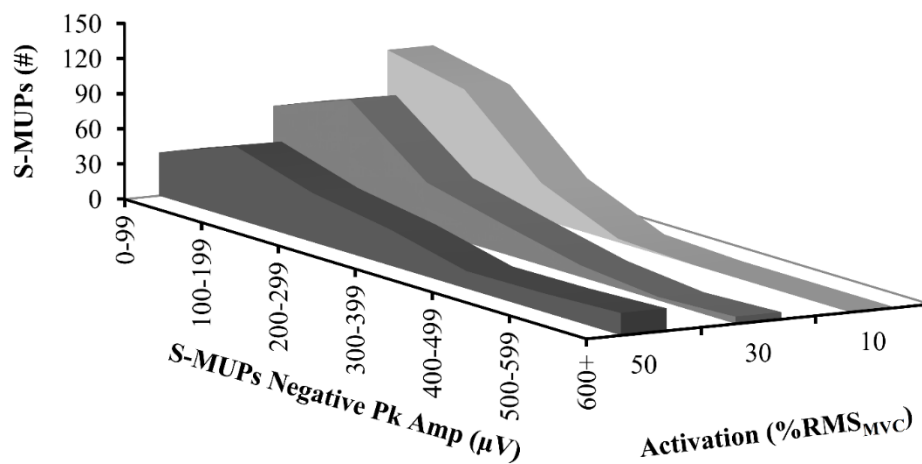


Figure 6. Frequency distribution histograms of S-MUP negative-peak amplitudes (Negative Pk Amp) at three relative muscle activation levels (10%, 30%, 50% RMS_{MVC}). #, number; RMS_{MVC} , root-mean-square of anconeus EMG during maximal voluntary contraction (MVC) of the elbow extensors.

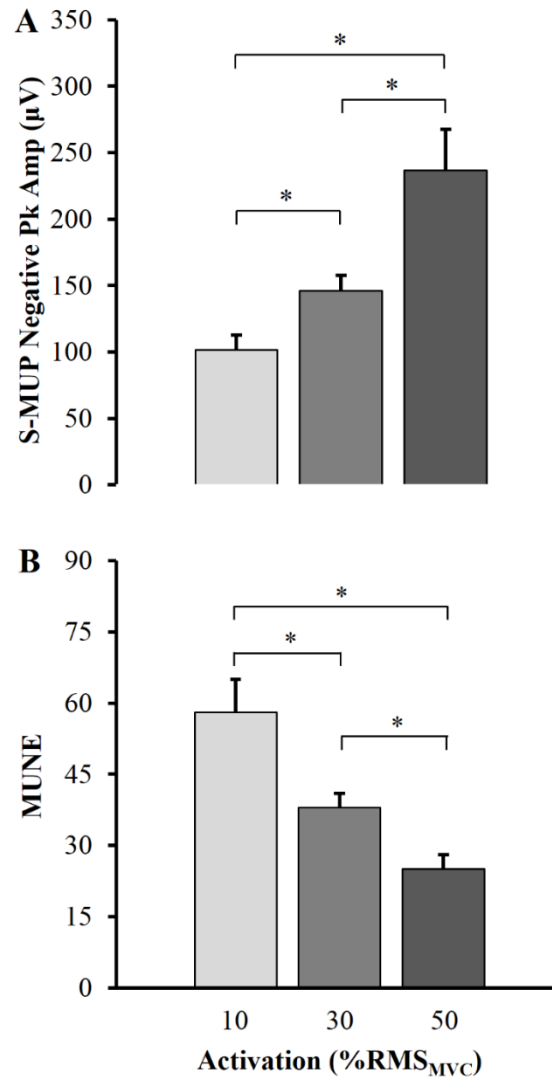


Figure 7. A) Average surface detected motor unit potentials (S-MUPs) and B) derived motor unit number estimates (MUNEs) at three target activation levels (10%, 30%, and 50%RMS_{MVC}). Data are presented as mean \pm SE. * denotes difference among muscle activations ($P < 0.05$). Negative Pk Amp, negative-peak amplitude, RMS_{MVC}, root-mean-square of anconeus EMG during maximal voluntary contraction (MVC) of the elbow extensors.

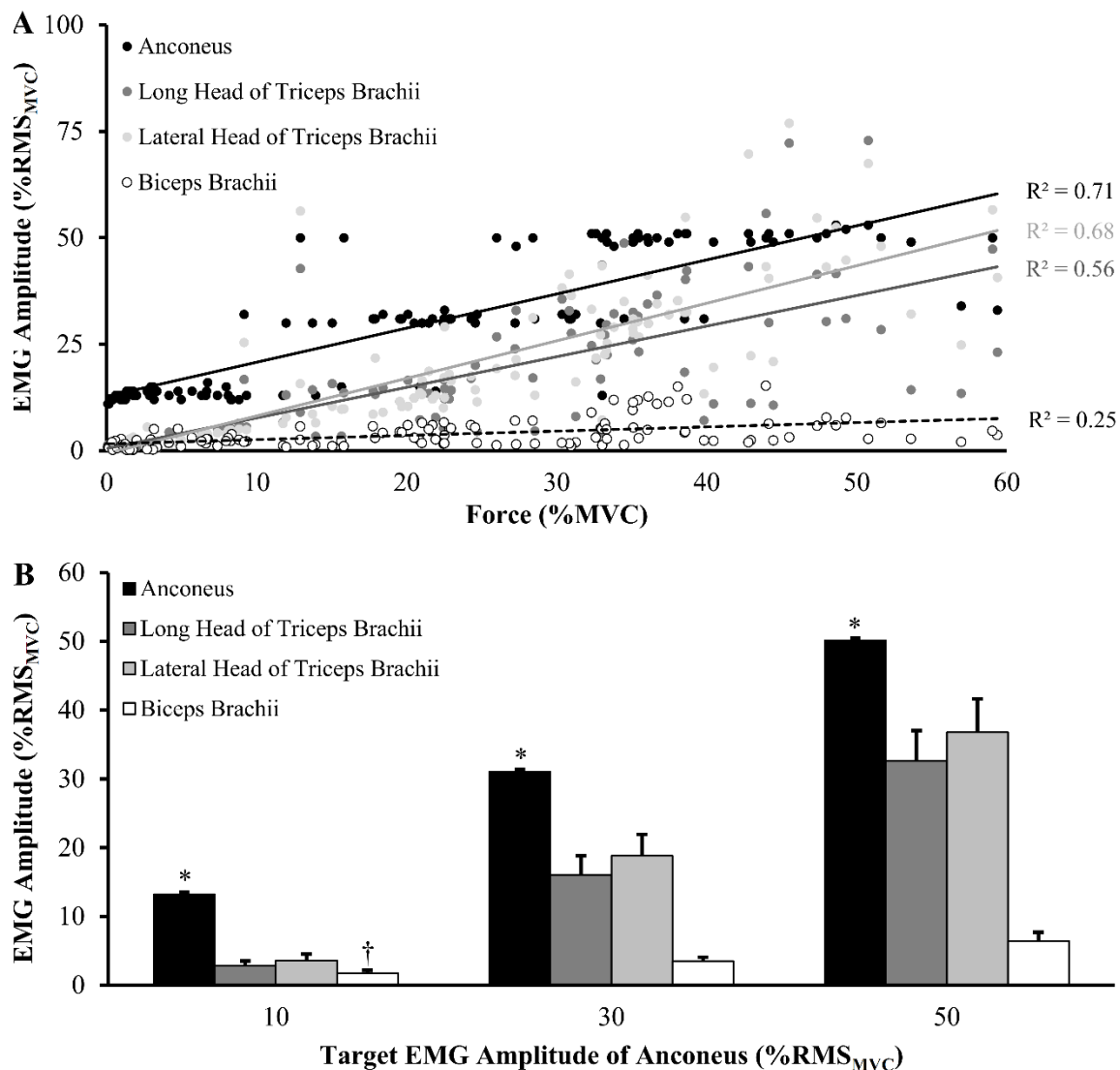


Figure 8. A) Scatterplot of force (%MVC) plotted against normalized EMG amplitude (%RMS_{MVC}) for anconeus (closed circles), long head of triceps brachii (dark grey circles), lateral head of triceps brachii (light grey circles), and biceps brachii (open diamonds) at three anconeus muscle activation levels (10%, 30%, and 50%RMS_{MVC}). Coefficients of determination for the least squares regression lines of the: anconeus, $R^2 = 0.71$; lateral head, $R^2 = 0.68$; long head of triceps brachii, $R^2 = 0.56$; and biceps brachii, $R^2 = 0.25$. B) Bar graph of target EMG amplitude of anconeus (%RMS_{MVC}) plotted against normalized EMG amplitude (%RMS_{MVC}) for anconeus (black bars), long head of

triceps brachii (dark grey bars), lateral head of triceps brachii (light grey bars), and biceps brachii (white bars). Data are presented as mean \pm SE. * denotes difference between anconeus and long and lateral heads of the triceps brachii within a target EMG amplitude ($P < 0.05$). † denotes biceps brachii EMG coactivation is significantly greater between 10% and 50% RMS_{MVC} . RMS_{MVC} , root-mean-square of anconeus EMG during maximal voluntary contraction (MVC) of the elbow extensors.

3.4 DISCUSSION

These results, in keeping with the size principle of orderly recruitment (Henneman et al., 1965), indicate that larger MUs are recruited at higher levels of muscle activation as evidenced by higher average S-MUP negative-peak amplitudes at increased activation levels. Relative to the CMAP, the larger S-MUPs at higher activation levels resulted in correspondingly lower MUNE. This negative relationship between S-MUP amplitude and MUNE has been reported previously in the tibialis anterior (McNeil et al., 2005; Power et al., 2010), first dorsal interosseus (FDI) (Boe et al., 2005), soleus (Dalton et al., 2008), and biceps brachii (Power et al., 2012). However, in all these models, successful MUNE was limited to contraction intensities $\leq 40\%MVC$, falling below the upper limits of MU recruitment in these muscles (Seki and Narusawa, 1996; Van Cutsem et al., 1997; Oya et al., 2009). The inability to explore contraction intensities $>40\%MVC$ was the result of limitations in DE-STA software; specifically the inability to decompose MU potentials from a complex and stochastic EMG signal, when an increased number of MUs contributes to the interference pattern. Here, because of the unique aspects of the anconeus outlined in the introduction, we were able to test this relationship at higher activations ($50\%RMS_{MVC}$) and, most importantly, perform MUNE with DE-STA at a muscle activation level which presumably recruited a sample-representative of the whole MU pool for this muscle (Harwood et al., 2012b).

The frequency histograms indicated that $50\%RMS_{MVC}$ yielded the most physiological distribution of negative-peak S-MUP amplitudes across the broadest range ($31-1205\mu V$) of available MUs relative to $10\%RMS_{MVC}$ ($18-341\mu V$) and $30\%RMS_{MVC}$ ($18-902\mu V$); it therefore better represents the activation of the whole MU pool in this

muscle. Moreover, repositioning of the indwelling needle electrode allowed sampling of a variety of MUs with correspondingly different sized S-MUPs from the whole MU pool, further increasing the likelihood of a MUNE which is more representative of the entire muscle. We found relatively few MUs for the anconeus (38 at 30% RMS_{MVC} , equivalent to an average elbow extension force of 25%MVC) compared with other small limb muscles such as the FDI (91 at 30%MVC) (Boe et al., 2005), likely contributing to less signal interference, thus allowing the DE-STA technique to estimate MU numbers at higher muscle activations. The relatively few MUs estimated for the anconeus likely reflect the function of the muscle rather than simply the small size. Functionally, the anconeus is considered to be an accessory elbow extensor and stabilizer involved in gross movement control. The FDI, which is significantly smaller ($\sim 180\text{mm}^2$ vs $\sim 250\text{mm}^2$ for the anconeus) (An et al., 1981; Infantolino and Challis, 2011), is critically involved in fine skilled hand movements and has 6-8 times more estimated numbers of MUs than the anconeus (Boe et al., 2005). Moreover, the abductor hallucis, which performs simple large toe abduction, is similar in size to the anconeus ($\sim 270\text{mm}^2$) (Cameron et al., 2008), and also has relatively few MUs (ranging from 10-70) (Johns and Fuglevand, 2011). Thus, given the function in relation to the size of the anconeus, it is perhaps not surprising to estimate low numbers of MUs.

Muscle activations (% RMS_{MVC}) for the elbow extensors and overall elbow extensor force (%MVC) during isometric elbow extension contractions were recorded to examine the neuromuscular function of the anconeus and its role in contributing to elbow extension. In general, the force-EMG relationship appears to depend highly upon the histophysiology of the muscle or muscle portion under investigation. Specifically, the

degree to which MU recruitment and rate coding contribute to force production, as a result of the diversity of MU sizes in the muscle (Fuglevand et al., 1993; Lawrence and DeLuca et al., 1983) and the interaction of synergistic muscles to accomplish a coordinated task. Linear force-EMG relationships are observed generally in muscles comprised of a variety of MU sizes, because force production is dependent upon a combination of recruitment and rate coding, whereas non-linear relationships are common in muscles with predominately similar sized MUs (Fuglevand et al., 1993; Lawrence and DeLuca et al., 1983). We observed a strong linear relationship between force (%MVC) and EMG amplitude (%RMS_{MVC}) for the anconeus and for the lateral and long heads of the triceps brachii (Figure 8A), suggesting both MU recruitment and rate coding contribute overall to elbow extensor force gradation. However, the slope and y-axis offset of the least squares regression lines differed among muscles, whereby the lateral and long heads of the triceps brachii exhibited almost no muscle activation at 10%RMS_{MVC} compared to the anconeus and failed to exceed anconeus EMG amplitudes across all elbow extension forces (Figure 8A). A commonly reported limitation for the DQEMG technique is the challenge of deriving MUNE_s at high target forces or high muscle activation levels (McNeil et al., 2005; Boe et al., 2005). As a consequence, MUNE_s cannot be assumed to always represent the entire MU pool or “true anatomical number”, especially in muscles that grade force predominantly through MU recruitment. The high level of anconeus muscle activation recorded by surface EMG at low elbow extension forces and more gradual increases in EMG amplitude compared with the heads of the triceps brachii at higher forces indicates the anconeus relies more on MU recruitment at low forces (Le Bozec and Maton, 1982; Le Bozec et al., 1980), whereas,

rate coding predominates at forces above ~25-35%MVC (Harwood et al., 2012b). Conversely, as outlined in the introduction, modulation of force has been reported over a larger range of elbow extension intensities primarily through increases in MU recruitment in the triceps brachii (Dalton et al., 2010; Harwood and Rice, 2012). Additionally, relatively high anconeus muscle activation at low force production supports the role of the anconeus as an elbow stabilizer (Dideriksen et al., 2012). Nevertheless, during the task of increasing levels of elbow extension, the anconeus continues to contribute to force production accordingly (Figure 8A & B) and therefore participates in attainment of maximum elbow extension force. Thus, from a clinical perspective the anconeus is a suitable muscle for investigation of MUNE, as MU action potentials can be recorded at high muscle activation levels in which it seems likely the majority of MUs are active. As a result, the random sample of MUs used to derive the MUNE is more representative of the entire pool of MUs and not biased towards lower threshold MUs as it might be in rate coding oriented muscles.

In summary, a progressive increase in mean S-MUP negative-peak amplitude and subsequent decrease in MUNE was observed with increasing muscle activation levels in the anconeus. The anconeus as a model allowed for MUNE at higher levels of muscle activations ($50\%RMS_{MVC}$), which has not been feasible in other muscles tested using DE-STA. The force-EMG relationships of the anconeus, compared with the lateral and long heads of the triceps brachii, indicate that most, if not all, MUs in the muscle are recruited at $50\%RMS_{MVC}$, such that a sample of the overall MU pool was taken, yielding a MUNE which seems most representative of the number and sizes of MUs in this muscle. Furthermore, the results indicate the anconeus has a low number of MUs when compared

to other small limb muscles (e.g., hand muscles), which may be one reason for the success in discriminating individual MUs at novel intensities of effort ($50\%RMS_{MVC}$) and very fast elbow extensions (Harwood et al., 2011). The effect of muscle activation on MUNE demonstrated here and those reported previously (McNeil et al., 2005; Boe et al., 2004; 2009; 2005), suggest that muscle activation levels should be recognized when conducting MUNE studies. The unique properties of the anconeus highlighted here indicate that it may be a useful model to explore changes in MUNE and MU properties in health and disease.

3.5 REFERENCES

- Abellaneda S, Guissard N, Duchateau J. The relative lengthening of the myotendinous structures in the medial gastrocnemius during passive stretching differs among individuals. *J Appl Physiol* 2009; 106:169-177.
- An K, Hui FC, Morrey BF, Linscheid RL, Chao EY. Muscles across the elbow joint: a biomechanical analysis. *J Biomech* 1981; 14(10):659-669.
- Basmajian JV, Griffin WR. Function of anconeus muscle. An electromyographic study. *J Bone Joint Surg Am* 1972; 54:1712-1714.
- Belanger AY, McComas AJ. Extent of motor unit activation during effort. *J Appl Physiol* 1981; 51:1131-5.
- Boe SG, Dalton BH, Harwood B, Doherty TJ, Rice CL. Inter-rater reliability of motor unit number estimates and quantitative motor unit analysis in the tibialis anterior muscle. *Clin Neurophysiol* 2009; 120:947-952.
- Boe SG, Stashuk DW, Brown WF, Doherty TJ. Decomposition-based quantitative electromyography: effect of force on motor unit potentials and motor unit number estimates. *Muscle Nerve* 2005; 31:365-373.
- Boe SG, Stashuk DW, Doherty TJ. Motor unit number estimation by decomposition-enhanced spike-triggered averaging: control data, test-retest reliability, and contractile level effects. *Muscle Nerve* 2004; 29:693-699.
- Boe SG, Stashuk DW, Doherty TJ. Within-subject reliability of motor unit number estimates and quantitative motor unit analysis in a distal and proximal upper limb muscle. *Clin Neurophysiol* 2006; 117:596-603.

- Bromberg MB, Brownell AA. Motor unit number estimation in the assessment of performance and function in motor neuron disease. *Phys Med Rehabil Clin N Am* 2008; 19:509-532.
- Bromberg MB. Updating motor unit number estimation (MUNE). *Clin Neurophysiol* 2007; 118:1-8.
- Cameron AF, Rome K, Hing WA. Ultrasound evaluation of the abductor hallucis muscle: reliability study. *J Foot Ankle Res* 2008; 1:1-12.
- Coriolano MD, Amoriom Jr AA, Lins OG. Repetitive stimulation test on the anconeus muscle for the diagnosis of myasthenia gravis: the mapping of its motor end-plate area. *Arq Neuropsiquiatr* 2007; 65(2B):488-491.
- Dalton BH, Jakobi JM, Allman BL, Rice CL. Differential age-related changes in motor unit properties between elbow flexors and extensors. *Acta Physiol (Oxf)* 2010; 200(1):45-55.
- Dalton BH, McNeil CJ, Doherty TJ, Rice CL. Age-related reductions in the estimated numbers of motor units are minimal in the human soleus. *Muscle Nerve* 2008; 38:1108-1115.
- Daube JR, Sorenson EJ, Windebank AJ. Prospective 15-year study of neuromuscular function in a cohort of patients with prior poliomyelitis. *Suppl Clin Neurophysiol* 2009; 60:197-201.
- Davidson AW, Rice CL. Effect of shoulder angle on the activation pattern of the elbow extensors during a submaximal isometric fatiguing contraction. *Muscle Nerve* 2010; 42(4):514-521.

- Dideriksen JL, Negro F, Enoka RM, Farina D. Motor unit recruitment strategies and muscle properties determine the influence of synaptic noise on force steadiness. *J Neurophysiol* 2012; 107(12):3357-3369.
- Doherty TJ, Stashuk DW, Boe SG. Decomposition-enhanced spike triggered averaging MUNE: validity, reliability, and impact of contraction force. *Suppl Clin Neurophysiol* 2009; 60:119-127.
- Doherty TJ, Stashuk DW. Decomposition-based quantitative electromyography: methods and initial normative data in five muscles. *Muscle Nerve* 2003; 28:204-211.
- Fuglevand AJ, Winter DA, Patla AE. Models of recruitment and rate coding organization in motor-unit pools. *J Neurophysiol* 1993; 70(6):2470-2488.
- Gassel MM, Diamantopoulos E. Pattern of conduction times in the distribution of the radial nerve. *Neurology* 1964; 14:222-231.
- Harwood B, Choi IH, Rice CL. Reduced motor unit discharge rates of maximal velocity dynamic contractions in response to a submaximal dynamic fatigue protocol. *J Appl Physiol* 2012a; 113(12):1821-1830.
- Harwood B, Dalton BH, Power GA, Rice CL. Muscle-dependent motor unit recruitment behaviour of the elbow extensors. Program No. 887.23. 2012b Neuroscience Meeting Planner. New Orleans, LA: Society for Neuroscience, 2012b. Online.
- Harwood B, Davidson AW, Rice CL. Motor unit discharge rates of the anconeus muscle during high-velocity elbow extensions. *Exp Brain Res* 2011; 208:103-113.
- Harwood B, Rice CL. Changes in motor unit recruitment thresholds of the human anconeus muscle during torque development preceding shortening elbow extensions. *J Neurophysiol* 2012; 107(10):2876-2884.

- Henneman E, Somjen G, Carpenter DO. Excitability and inhibitability of motoneurons of different sizes. *J Neurophysiol* 1965; 28(3):599-620.
- Hwang K, Han JY, Chung IH. Topographical anatomy of the anconeus muscle for use as a free flap. *J Reconstr Microsurg* 2004; 20:631-636.
- Infantolino BW, Challis JH. Estimating the volume of the first dorsal interosseus using ultrasound. *Med Eng Phys* 2011; 33(3):391-394.
- Johns RK, Fuglevand AJ. Number of motor units in human abductor hallucis. *Muscle Nerve* 2011; 43:895-896.
- Kennett RP and Fawcett PRW. Repetitive nerve stimulation of anconeus in the assessment of neuromuscular transmission disorders. *Electroencephalogr Clin Neurophysiol* 1993; 89:170-176.
- Lawrence JH, De Luca CJ. Myoelectric signal versus force relationship in different human muscles. *J Appl Physiol* 1983; 54(6):1653–1659.
- Le Bozec S, Maton B, Cnockaert JC. The synergy of elbow extensor muscles during static work in man. *Eur J Appl Physiol Occup Physiol* 1980; 43(1):57-68.
- Le Bozec S, Maton B. The activity of anconeus during voluntary elbow extension: the effect of lidocaine blocking of the muscle. *Electromyogr Clin Neurophysiol* 1982; 22(4):265-75.
- Maselli RA, Mass DP, Distad BJ, Richman DP. Anconeus muscle: a human muscle preparation suitable for in-vitro microelectrode studies. *Muscle Nerve* 1991; 14:1189-1192.

McNeil CJ, Doherty TJ, Stashuk DW, Rice CL. The effect of contraction intensity on motor unit number estimates of the tibialis anterior. *Clin Neurophysiol* 2005; 116:1342-1347.

Naito A, Shimizu Y, Handa Y, Ichie M, Hoshimiya N. Functional anatomical studies of the elbow movements. I. Electromyographic (EMG) analysis. *Okajimas Folia Anat Jpn* 1991; 68(5):283-288.

Olney RK, Lomen-Hoerth C. Motor unit number estimation (MUNE): how may it contribute to the diagnosis of ALS? *Amyotroph Lateral Scler Other Motor Neuron Disord* 2000; 2:S41-44.

Oya T, Riek S, Cresswell, AG. Recruitment and rate coding organisation for soleus motor units across entire range of voluntary isometric plantar flexion. *J Physiol* 2009; 587(19):4737-4748.

Pasquet B, Carpentier A, Duchateau J. Specific modulation of motor unit discharge for a similar change in fascicle length during shortening and lengthening contractions in humans. *J Physiol* 2006; 577:753-765.

Pereira BP. Revisiting the anatomy and biomechanics of the anconeus muscle and its role in elbow stability. *Ann Anat* 2013; 195(4):365-370.

Power GA, Dalton BH, Behm DG, Doherty TJ, Vandervoort AA, Rice CL. Motor unit survival in lifelong runners is muscle dependent. *Med Sci Sports Exerc* 2012; 44(7):1235-1242.

Power GA, Dalton BH, Behm DG, Vandervoort AA, Doherty TJ, Rice CL. Motor unit number estimates in masters runners: use it or lose it? *Med Sci Sports Exerc* 2010; 42(9):1644-1650.

- Seki L, Narusawa M. Firing rate modulation of human motor units in different muscles during isometric contraction with various forces. *Brain Res* 1996; 719(1-2):1-7.
- Sorenson EJ, Daube JR, Windebank AJ. Motor unit number estimates correlate with strength in polio survivors. *Muscle Nerve* 2006; 34(5):608-613.
- Stashuk DW, Doherty TJ, Brown WF. MUNE using decomposition-enhanced spike-triggered averaging. *Clin Physiol* 2003; 55:108-121.
- Travill AA. Electromyographic study of the extensor apparatus of the forearm. *Anat Rec* 1962; 144:373-376.
- Van Cutsem M, Feiereisen P, Duchateau J, Hainaut K. Mechanical properties and behaviour of motor units in the tibialis anterior during voluntary contractions. *Can J Appl Physiol* 1997; 22(6):585-597.
- Zhang LQ, Nuber GW. Moment distribution among human elbow extensor muscles during isometric and submaximal extension. *J Biomech* 2000; 33:145-154.

4.0 GENERAL DISCUSSION AND SUMMARY

The studies presented in Chapters 2 and 3 of this thesis investigate the functional anatomy of the anconeus in healthy young men. The specific aim was to examine anconeus anatomy as it pertains to its role as a valuable model in the study of motor unit (MU) properties (Harwood et al., 2011; 2012a; 2013). To achieve this, ultrasonography and decomposition-enhanced spike-triggered averaging (DE-STA) were used to explore muscle architecture and functional MU numbers in the anconeus, respectively.

The main findings of this thesis are that anconeus muscle architecture, specifically fascicle length (L_F) and pennation angle (PA), is dynamic, undergoing substantial changes with elbow joint excursion that are similar to other limb muscles reported elsewhere (Blazevich et al., 2001; Kubo et al., 2003; Kawakami et al., 1993; Kawakami et al., 1998; Chleboun et al., 2001; Fukunaga et al., 1997). The values obtained here are more representative of architectural changes at various elbow joint positions than those reported in cadaveric studies (Coriolano et al., 2009; Pereira, 2013; Ng et al., 2012). Furthermore, understanding these anatomical features relates to aspects of motor control related to MU recruitment and rate coding (Pasquet et al., 2005), but do not directly explain the clarity of intramuscular electromyography (EMG) previously reported. In Chapter 3, MU number estimates (MUNE) were successfully derived using DE-STA at higher muscle activation levels (root-mean-square of maximum voluntary contraction (RMS_{MVC})) than previously reported in other limb muscles (Boe et al., 2005; McNeil et al., 2005; Dalton et al., 2008; Power et al., 2010). Surface-detected MU potential distribution and elbow extensor force-EMG data indicate near or full MU recruitment at $50\%RMS_{MVC}$, yielding a MUNE which is representative of the entire MU pool.

Furthermore, the anconeus has a relatively low number of MUs compared to other small limb muscles (e.g., hand muscles) (Boe et al., 2005), which may explain the ability to discriminate individual MUs at higher intensities of effort ($50\%RMS_{MVC}$) than previously reported. In conclusion, the high signal-to-noise ratio that has made the anconeus a choice model in the study of MU properties, is more likely attributed to a relatively low number of MUs than minimal absolute change in its muscle architecture with elbow joint excursion.

4.1 LIMITATIONS

A general limitation of the anconeus is that elbow extension is the main movement that activates it, and although active at all levels, the anconeus only contributes $\sim 15\%$ to maximum elbow extension torque. Thus, other than relative EMG measures ($\%RMS_{MVC}$), it is difficult to appreciate its contribution to extension torque which may limit this muscle for studies related to aging, training, and fatigue.

The results from Chapter 2 concluded that L_F and PA decreased and increased, respectively, with elbow joint extension. These measures were made at five angles under static, passive conditions, as ultrasound imaging of the anconeus is not without limitation. Efforts were made to follow a change in muscle architecture during continuous slow, low intensity contractile movement, and at static angles during various contractile intensities. However, measurement of L_F and PA change during dynamic movement proved very difficult, a result of the relatively small size and challenging location of the anconeus (just spanning the elbow joint). Similarly, isometric contractions with force enough to cause visible internal shortening of the muscle resulted in probe displacement, precluding the continuous image capture of the target fascicles. Thus, as a model, the anconeus

poses a challenge when measuring contractile or dynamic contraction-induced changes in muscle architectural features.

In general, DE-STA derived MUNE_s have been limited to low or moderate contraction intensities (McNeil et al., 2005; Dalton et al., 2008; Boe et al., 2005; Power et al., 2010), as higher intensities result in complex and stochastic EMG signals that are not readily decomposed by the computer software (Boe et al., 2005; Conwit et al., 1997). However, in Chapter 3, unique properties of the anconeus allowed for successful MUNE_s at a novel, higher muscle activation level ($50\%RMS_{MVC}$). The $50\%RMS_{MVC}$ target level was equivalent to $\sim 40\%MVC$ of the elbow extensors, which according to previous research exceeds MU recruitment for this muscle ($\sim 25\text{-}35\%MVC$) (Harwood et al., 2012b), providing a MUNE that is representative of its entire MU pool. Therefore, contraction intensity was not a limiting factor with the anconeus, as target levels beyond $50\%RMS_{MVC}$ would likely only contribute to greater EMG signal interference and a less reliable MUNE.

4.2 FUTURE DIRECTIONS

Although these studies have advanced our knowledge of anconeus functional anatomy, some questions still remain. In Chapter 2, ultrasound images were only successfully obtained at rest, under passive conditions due to limitations associated with the ultrasonography technique used. Flat ultrasound probes that can be secured over the muscle of interest, may have enabled image collection during dynamic movements or at low contractile intensities for this muscle, as they have proven beneficial in the observation of fascicle lengths during activities such as walking and running (Aggelousis et al., 2010). Furthermore, extended field-of-view imaging and tracking software might

allow for greater ease when attempting to follow muscle fascicles under active and dynamic conditions. If these improvements in the imaging technique were successful, then it would be of significant interest to examine the effect of L_F and PA change on MU recruitment and discharge rate during isometric and dynamic contractions at various intensities or levels of muscle activation. This would aid in understanding the mechanisms behind force production at different muscle lengths.

Lastly, Chapter 3 investigated the number of functional MUs in the anconeus. The ability to ascertain a MUNE at a muscle activation which recruits the entire MU pool, as was done here, could have beneficial application in the study of aging and disease. Numerous studies have explored MU loss with disease (i.e., ALS, diabetes) (Boe et al., 2009; Allen et al., 2013) and aging (Dalton et al., 2008; Power et al., 2010; 2012). However, EMG signal interference limited these studies to contractile intensities $\leq 40\%MVC$, which likely did not equal or exceed the upper limit of MU recruitment for the muscle under investigation. Therefore, anconeus MUNE_s obtained at $50\%RMS_{MVC}$ could provide further insight into the effect of aging and disease on higher threshold MUs, although as noted above the model has some limitations. Furthermore, previous clinical applications (Kennett and Fawcett, 1993), as well as the current study, found radial nerve stimulation and needle EMG to be very tolerable in the anconeus, suggesting it is an attractive model for study in aged and diseased populations.

With virtually all limb muscles, *in vivo* study is a compromise between selecting the most appropriate muscle model for the research question and that which has minimal functional and technical limitations. We cannot change the anatomy or become more

invasive but likely future technical improvements in imaging and EMG will allow further understanding of neuromuscular structure and function *in vivo*.

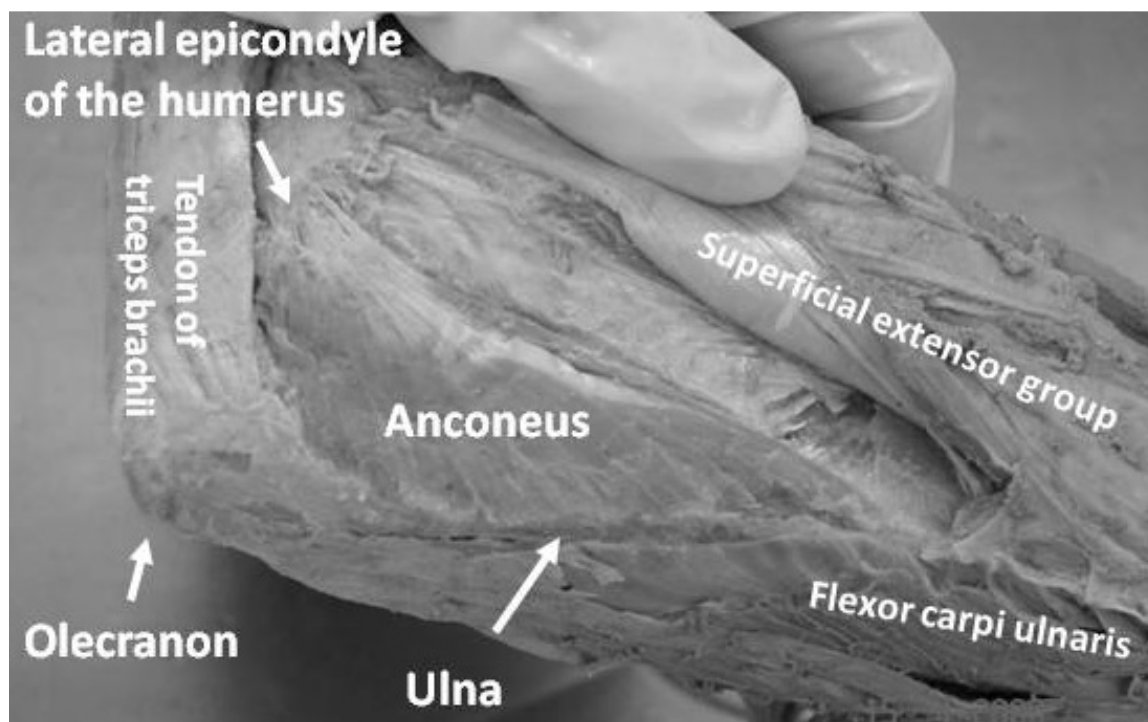
4.3 REFERENCES

- Aggeloussis N, Giannakou E, Albracht K, Arampatzis. Reproducibility of fascicle length and pennation angle of gastrocnemius medialis in human gait in vivo. *Gait Posture* 2010; 31:73-77.
- Allen MD, Choi IH, Kimpinski K, Doherty TJ, Rice CL. Motor unit loss and weakness in association with diabetic neuropathy in humans. *Muscle Nerve* 2013; 48(2):298-300.
- Blazevich AJ, Giorgi A. Effect of testosterone administration and eight training on muscle architecture. *Med Sci Sports Exerc* 2001; 33(1):1688-1693.
- Boe SG, Stashuk DW, Brown WF, Doherty TJ. Decomposition-based quantitative electromyography: effect of force on motor unit potentials and motor unit number estimates. *Muscle Nerve* 2005; 31:365-373.
- Boe SG, Stashuk DW, Doherty TJ. Motor unit number estimates, quantitative motor unit analysis and clinical outcome measures in amyotrophic lateral sclerosis. *Suppl Clin Neurophysiol* 2009; 60:181-189.
- Chleboun GS, France AR, Crill MT, Braddock HK, Howell JN. In vivo measurement of fascicle length and pennation angle of the human biceps femoris muscle. *Cells Tissues Organs* 2001; 169(4):401-409.
- Conwit RA, Tracy B, Jamison C, McHugh M, Stashuk D, Brown WF, Metter EJ. Decomposition-enhanced spike-triggered averaging: contraction level effects. *Muscle Nerve* 1997; 20(8):976-982.
- Coriolano MGWS, Lins OG, Amorim MJAAL, Amorim AA. Anatomy and functional architecture of the anconeus muscle. *Int J Morph* 2009; 27(4):1009-1012.

- Dalton BH, McNeil CJ, Doherty TJ, Rice CL. Age-related reductions in the estimated numbers of motor units are minimal in the human soleus. *Muscle Nerve* 2008; 38:1108-1115.
- Fukunaga T, Ichinose Y, Ito M, Kawakami Y, Fukashiro S. Determination of fascicle length and pennation in a contracting human muscle in vivo. *J Appl Physiol* 1997; 82(1):354-358.
- Harwood B, Choi IH, Rice CL. Reduced motor unit discharge rates of maximal velocity dynamic contractions in response to a submaximal dynamic fatigue protocol. *J Appl Physiol* 2012a; 113(12):1821-1830.
- Harwood B, Dalton BH, Power GA, Rice CL. Motor unit properties from three synergistic muscles during ramp isometric elbow extensions. *Exp Brain Res* 2013; 231(4):501-510.
- Harwood B, Dalton BH, Power GA, Rice CL. Muscle-dependent motor unit recruitment behaviour of the elbow extensors. Program No. 887.23. 2012b Neuroscience Meeting Planner. New Orleans, LA: Society for Neuroscience, 2012b. Online.
- Harwood B, Davidson AW, Rice CL. Motor unit discharge rates of the anconeus muscle during high-velocity elbow extensions. *Exp Brain Res* 2011; 208:103-113.
- Kawakami Y, Abe T, Fukunaga T. Muscle-fiber pennation angles are greater in hypertrophied than in normal muscles. *J Appl Physiol* 1993; 74(6):2740-2744.
- Kawakami Y, Ichinose Y, Fukunaga T. Architectural and functional features of human triceps surae muscles during contraction. *J Appl Physiol* 1998; 85(2):398-404.

- Kennett RP, Fawcett PR. Repetitive nerve stimulation of anconeus in the assessment of neuromuscular transmission disorders. *Electroencephalogr Clin Neurophysiol* 1993; 89(3):170-176.
- Kubo K, Kanehisa H, Azuma K, Ishizu M, Kuno SY, Okada M, Fukunaga T. Muscle architectural characteristics in young and elderly men and women. *Int J Sports Med* 2003; 24(2):125-130.
- McNeil CJ, Doherty TJ, Stashuk DW, Rice CL. The effect of contraction intensity on motor unit number estimates of the tibialis anterior. *Clin Neurophysiol* 2005; 116:1342-1347.
- Pasquet B, Carpentier A, Duchateau J. Change in muscle fascicle length influences the recruitment and discharge rate of motor units during isometric contractions. *J Neurophysiol* 2005; 94(5):3126-3133.
- Pereira BP. Revisiting the anatomy and biomechanics of the anconeus muscle and its role in elbow stability. *Ann Anat* 2013; 195(4):365-370.
- Power GA, Dalton BH, Behm DG, Doherty TJ, Vandervoort AA, Rice CL. Motor unit survival in lifelong runners is muscle dependent. *Med Sci Sports Exerc* 2012; 44(7):1235-1242.
- Power GA, Dalton BH, Behm DG, Vandervoort AA, Doherty TJ, Rice CL. Motor unit number estimates in masters runners: use it or lose it? *Med Sci Sports Exerc* 2010; 42(9):1644-1650.

APPENDIX A



(Coriolano et al., 2009)

APPENDIX B



Use of Human Participants - Ethics Approval Notice

Principal Investigator: Dr. Charles Rice
Review Number: 18097
Review Level: Full Board
Approved Local Adult Participants: 100
Approved Local Minor Participants: 0
Protocol Title: Neuromuscular control of human movement
Department & Institution: Anatomy & Cell Biology, University of Western Ontario
Sponsor: Natural Sciences and Engineering Research Council

Ethics Approval Date: July 22, 2011

Expiry Date: August 31, 2015

Documents Reviewed & Approved & Documents Received for Information:

Document Name	Comments	Version Date
UWO Protocol		
Letter of Information & Consent		

This is to notify you that the University of Western Ontario Health Sciences Research Ethics Board (HSREB) which is organized and operates according to the Tri-Council Policy Statement: Ethical Conduct of Research Involving Humans and the Health Canada/ICH Good Clinical Practice Practices: Consolidated Guidelines; and the applicable laws and regulations of Ontario has reviewed and granted approval to the above referenced study on the approval date noted above. The membership of this HSREB also complies with the membership requirements for REB's as defined in Division 5 of the Food and Drug Regulations.

The ethics approval for this study shall remain valid until the expiry date noted above assuming timely and acceptable responses to the HSREB's periodic requests for surveillance and monitoring information. If you require an updated approval notice prior to that time you must request it using the UWO Updated Approval Request form.

Member of the HSREB that are named as investigators in research studies, or declare a conflict of interest, do not participate in discussions related to, nor vote on, such studies when they are presented to the HSREB.

The Chair of the HSREB is Dr. Joseph Gilbert. The UWO HSREB is registered with the U.S. Department of Health & Human Services under the IRB registration number IRB 00000940.

Signature

Ethics Officer to Contact for Further Information

<input checked="" type="checkbox"/> Janice Sutherland	<input type="checkbox"/> Grace Kelly	<input type="checkbox"/> Shantel Walcott
-------------------------------------------------------	--------------------------------------	------------------------------------------

This is an official document. Please retain the original in your files.

The University of Western Ontario

Office of Research Ethics

Support Services Building Room 5150 • London, Ontario • CANADA - N6A 3K7
 PH: 519-661-3036 • F: 519-850-2466 • ethics@uwo.ca • www.uwo.ca/research/ethics

APPENDIX C

RightsLink - Your Account

Page 1 of 5

JOHN WILEY AND SONS LICENSE TERMS AND CONDITIONS

Feb 04, 2014

This is a License Agreement between Daniel E Stevens ("You") and John Wiley and Sons ("John Wiley and Sons") provided by Copyright Clearance Center ("CCC"). The license consists of your order details, the terms and conditions provided by John Wiley and Sons, and the payment terms and conditions.

All payments must be made in full to CCC. For payment instructions, please see information listed at the bottom of this form.

License Number	3322060180895
License date	Feb 04, 2014
Licensed content publisher	John Wiley and Sons
Licensed content publication	Muscle and Nerve
Licensed content title	Anconeus motor unit number estimates using decomposition-based quantitative electromyography
Licensed copyright line	Copyright © 2013 Wiley Periodicals, Inc., a Wiley company
Licensed content author	Daniel E.S. Stevens, Brad Harwood, Geoffrey A. Power, Timothy J. Doherty, Charles L. Rice
Licensed content date	Oct 10, 2013
Start page	n/a
End page	n/a
Type of use	Dissertation/Thesis
Requestor type	Author of this Wiley article
Format	Print and electronic
Portion	Full article
Will you be translating?	No
Title of your thesis / dissertation	Functional Anatomy of the Anconeus: Muscle Architecture and Motor Unit Number Estimation
Expected completion date	Apr 2014
Expected size (number of pages)	80
Total	0.00 USD
Terms and Conditions	

TERMS AND CONDITIONS

This copyrighted material is owned by or exclusively licensed to John Wiley & Sons, Inc. or one of its group companies (each a "Wiley Company") or a society for whom a Wiley Company has exclusive publishing rights in relation to a particular journal (collectively "WILEY"). By clicking "accept" in connection with completing this licensing transaction, you agree that the following terms and conditions apply to this transaction (along with the billing and payment terms and conditions established by the Copyright Clearance Center Inc., ("CCC's Billing and Payment terms and conditions"), at the time that you opened your RightsLink account (these are available at any time at <http://myaccount.copyright.com>).

Terms and Conditions

1. The materials you have requested permission to reproduce (the "Materials") are protected by copyright.

<https://s100.copyright.com/MyAccount/viewPrintableLicenseDetails?ref=8833689b-3c6c...> 04/02/2014

CURRICULUM VITAE

Name: **DANIEL E. STEVENS**

Post-Secondary Education and Degrees: The University of Western Ontario
London, ON
2012-2014 M.Sc.
Kinesiology

The University of Ottawa
Ottawa, ON
2006-2010 B.Sc. Honours
Major in Biology; Minor in Health Science

Related Work Experience: Teaching Assistant
The University of Western Ontario
2012-2013

Honours and Awards:

2013	Faculty of Health Science Travel Award
2013	Ontario Graduate Scholarship
2013	The University of Western Ontario Research Scholarship
2013	Kinesiology Graduate Student Travel Award
2012	The University of Western Ontario Research Scholarship
2009-2010	Dean's Honour List
2006-2010	Cum Laude Honours

Publications:

STEVENS, D.E., HARWOOD, B., POWER G.A., DOHERTY, T.J., RICE, C.L. (2013).
Anconeus motor unit number estimates using decomposition-based quantitative electromyography. *Muscle Nerve*. doi: 10.1002/mus.24092.

Abstracts/Presentations:

- STEVENS, D.E.S., HARWOOD, B., POWER G.A., DOHERTY, T.J., RICE, C.L.**
(2013). The great potential(s) of anconeus motor units. *Society of Neuroscience*, San Diego, CA.
- STEVENS, D.E.S., HARWOOD, B., POWER G.A., DOHERTY, T.J., RICE, C.L.**
(2013). Motor unit number estimates (MUNE) of the anconeus muscle. *Med Sci Sports and Ex* (Suppl. 45, No. 5) S300. Indianapolis, IN.
- STEVENS, D.E.** (2013) Motor units of the anconeus: Intensity matters. *Exercise Neuroscience Group*, Oshawa, ON. June 13-14.
- POWER, G.A., MAKRAKOS, D.P., STEVENS, D.E., HERZOG, W., RICE, C.L., VANDERVOORT, A.A.** (2014). Shortening induced torque depression in old age: Implications for power loss in the elderly? *Proceedings of the XXIVth World Congress of Biomechanics*, Boston, MA. IN PRESS
- MAKRAKOS, D.P., POWER, G.A., STEVENS, D.E.S., RICE, C.L., VANDERVOORT, A.A.** (2014). Need for speed? The velocity-dependence of eccentric dorsiflexor strength in older men. *Med Sci Sports and Ex*. Orlando, FLA. IN PRESS.